AUG 1 0 1978

AEDC-TR-77-126

cy.3

CORRELATION OF EXPERIMENTAL AND THEORETICAL STEADY-STATE SPINNING MOTION FOR A CURRENT FIGHTER AIRPLANE USING ROTATION-BALANCE AERODYNAMIC DATA

T. F. Langham
ARO, Inc., a Sverdrup Corporation Company

PROPULSION WIND TUNNEL FACILITY
ARNOLD ENGINEERING DEVELOPMENT CENTER
AIR FORCE SYSTEMS COMMAND
ARNOLD AIR FORCE STATION, TENNESSEE 37389

July 1978

Final Report for Period 1 July 1976 — 30 June 1977

Approved for public release; distribution unlimited.

Property of U. S. Air Force
AEDC LIBRARY
F40600-77-C-0003

Prepared for

ARNOLD ENGINEERING DEVELOPMENT CENTER/DOTR
ARNOLD AIR FORCE STATION, TENNESSEE 37389

NOTICES
When U. S. Government drawings, specifications, or other data are used for any purpose other than a definitely related Government procurement operation, the Government thereby incurs no responsibility nor any obligation whatsoever, and the fact that the Government may have formulated, furnished, or in any way supplied the said drawings, specifications, or other data, is not to be regarded by implication or otherwise, or in any manner licensing the holder or any other person or corporation, or conveying any rights or permission to manufacture, use, or sell any patented invention that may in any way be related thereto.
Qualified users may obtain copies of this report from the Defense Documentation Center.
References to named commerical products in this report are not to be considered in any sense as an indorsement of the product by the United States Air Force or the Government.

This report has been reviewed by the Information Office (OI) and is releasable to the National Technical Information Service (NTIS). At NTIS, it will be available to the general public, including foreign nations.

APPROVAL STATEMENT

This report has been reviewed and approved.

Alexander F. Money

ALEXANDER F. MONEY
Project Manager, Research Division
Directorate of Test Engineering

Approved for publication:

FOR THE COMMANDER

Marion L. Laster

MARION L. LASTER
Director of Test Engineering
Deputy for Operations

REPORT DOCUMENTATION PAGE		READ INSTRUCTIONS BEFORE COMPLETING FORM
1 REPORT NUMBER AEDC-TR-77-126	2 GOVT ACCESSION NO.	3. RECIPIENT'S CATALOG NUMBER
4 TITLE (and Subtitle) CORRELATION OF EXPERIMENTAL AND THEORETICAL STEADY-STATE SPINNING MOTION FOR A CURRENT FIGHTER AIRPLANE USING ROTATION-BALANCE AERODYNAMIC DATA		5 TYPE OF REPORT & PERIOD COVERED Final Report, 1 July 1976 - 30 June 1977 6 PERFORMING ORG. REPORT NUMBER
7 AUTHOR(s) T. F. Langham, ARO, Inc.		8 CONTRACT OR GRANT NUMBER(s)
9 PERFORMING ORGANIZATION NAME AND ADDRESS Arnold Engineering Development Center Air Force Systems Command Arnold Air Force Station, TN 37389		10 PROGRAM ELEMENT, PROJECT, TASK AREA & WORK UNIT NUMBERS Program Element 65807F
11 CONTROLLING OFFICE NAME AND ADDRESS Arnold Engineering Development Center (DOS) Air Force Systems Command Arnold Air Force Station, TN 37389		12. REPORT DATE July 1978 13 NUMBER OF PAGES 61
14 MONITORING AGENCY NAME & ADDRESS(if different from Controlling Office)		15. SECURITY CLASS. (of this report) UNCLASSIFIED 15a DECLASSIFICATION/DOWNGRADING SCHEDULE N/A

16 DISTRIBUTION STATEMENT (of this Report)

Approved for public release; distribution unlimited.

17 DISTRIBUTION STATEMENT (of the abstract entered in Block 20, if different from Report)

18 SUPPLEMENTARY NOTES

Available in DDC.

19. KEY WORDS (Continue on reverse side if necessary and identify by block number)

spinning (motion)
test methods
computerized simulation
decision making
models

20 ABSTRACT (Continue on reverse side if necessary and identify by block number)

An analytical study has been conducted to determine the usefulness of rotation-balance aerodynamic data in calculating the steady-state spin motion of a current fighter aircraft configuration. The analysis utilizes a nonlinear six-degree-of-freedom digital computer program to generate time histories of airplane spinning motion. Three aerodynamic data models were formulated and used in the spin analysis. The first model represents the

DD FORM 1 JAN 73 1473 EDITION OF 1 NOV 65 IS OBSOLETE

20. ABSTRACT (Continued)

conventional use of static and forced-oscillation data; the second model uses the static and forced-oscillation data but restricts the forced-oscillation data to that component of the total angular rate that is oscillatory; and the third model incorporates rotation-balance data from model 2 and restricts the rotation-balance data to that component of the total angular rate that is steady state. The results indicate a significantly different motion resulting from the three aerodynamic data models when compared to each other and to full-scale flight test steady-state spin motions. The motions produced by the rotation-balance aerodynamic model more closely simulate the motions exhibited during the flight tests.

AFSC
Arnold AFS Tenn

PREFACE

The work reported herein was conducted by the Arnold Engineering Development Center (AEDC), Air Force Systems Command (AFSC), under Program Element 65807F. The results of the research were obtained by ARO, Inc., AEDC Division (a Sverdrup Corporation Company), operating contractor for the AEDC, AFSC, Arnold Air Force Station, Tennessee, under ARO Project Number P32A-K4A. Analysis of the data was completed August 31, 1977, and the manuscript was submitted for publication on December 14, 1977.

The author wishes to acknowledge the contribution of R. W. Butler and W. C. Armstrong, ARO, Inc., who supported and aided the research effort.

CONTENTS

Page

1.0 INTRODUCTION 5
2.0 ANALYSIS
2.1 Description of Airplane 6
2.2 Aerodynamic Data 7
2.3 Method of Analysis 9
3.0 RESULTS AND DISCUSSION 10
4.0 CONCLUDING REMARKS 14
REFERENCES 15

ILLUSTRATIONS

Figure

1. Three-View Sketch of the F-4 Airplane 17
2. Rotation-Balance Apparatus 18
3. Comparison of Calculated Motions Using Aero Model 1 and Airplane Flight Motions 19
4. Comparison of Calculated Motions Using Aero Model 2 and Airplane Flight Motions 21
5.. Comparison of Calculated Motions Using Aero Model 3 and Airplane Flight Motions 23
6. Comparison of Calculated Motions for Aero Models 1 and 3, Left Pro-Spin Controls 25
7. Comparison of Calculated Motions Using Aero Model 3 with and without Forced-Oscillation Damping Data 27
8. Comparison of Calculated Motions Using Aero Model 3 System with $\Delta C_{\ell_{rb}}$ Only and Rotation-Balance Data 29
9. Comparison of Calculated Motions Using Aero Model 3 System with $\Delta C_{m_{rb}}$ Only and Rotation-Balance Data 31
10. Comparison of Calculated Motion Using Aero Model 3 System with $\Delta C_{n_{rb}}$ Only and Rotation-Balance Data 33
11. Comparison of NASA Ames and NASA Langley Static Normal-Force Coefficient, Controls Neutral Position 35
12. Comparison of NASA Ames and NASA Langley Static Pitching-Moment Coefficient, Controls Neutral Position 36

Figure Page

13. Comparison of Calculated Motions Using Aero Model 3 for Longitudinal Coefficient Increments 37
14. Comparison of Calculated Motions Using Aero Model 3 with and without Longitudinal Increments and Flight Test 39
15. Components of Flight Test Pitch Angular Acceleration 41
16. Variation of Aerodynamic Damping in Pitch with Angle of Attack 42
17. Comparison of Calculated Motions Using Aero Model 3 with and without Modifications in the Static and Pitch-Damping Data and Flight Test 43

TABLES

1. Mass, Inertia, and Dimensional Characteristics of the F-4 Aircraft 45
2. Initial Conditions from Flight 202, Run 12 of Ref. 12 46

APPENDIXES

A. EQUATIONS OF MOTION 47

B. IMPLEMENTATION METHODS FOR ROTATION-BALANCE DATA 52

C. DETERMINATION OF AERODYNAMIC MOMENTS FROM FLIGHT TEST. . 56

NOMENCLATURE 57

1.0 INTRODUCTION

The developed spin is classically defined as an equilibrium motion in which an airplane is descending toward earth at some angle of attack between stall and 90 deg while rotating about the vertical or near-vertical axis. The nature of this developed spin can be steady or oscillatory. From a pure definition sense, the steady spin occurs when the aerodynamic, inertial, and gyroscopic moments of the airplane are balanced. An oscillatory spin occurs when the moment equations of motion are not balanced and thus are simultaneously causing repetitive motions in both frequency and amplitude. The airplane flat spin is characterized as a steady spin and is accompanied by extreme angles of attack, high rotation rates, and small spin radius. In reality, those flight-experienced spins that are characterized as steady, flat spins are generally accompanied by a superposition of small oscillations in all rates and angles on the steady motions.

Flight experience has shown that the developed flat spin can be entered inadventently in high angle-of-attack maneuvers and that recovery can be difficult, if not impossible. For these reasons, much effort has been expended to better understand and predict airplane spin behavior.

Successful analytical simulation of airplane spinning motion has, in most cases, been achieved only after flight test data were acquired. With the aid of flight data, the aerodynamic data matrix is altered to provide good flight/simulator spin correlation. This after-the-fact adjustment is required because the true aerodynamics of the airplane spinning motion cannot be defined properly in conventional static wind tunnel testing. Large angular motions and separated flow conditions combine to produce nonlinearities in the aerodynamic forces and moments acting on the airplane in the spin. The severity of these nonlinearities is dependent on the configuration of the airplane and is the prime factor in determining the quantity of aerodynamic data required for accurate simulation of spinning motions.

Attempts to analytically model departure and spin entry characteristics using measured static and forced-oscillation aerodynamic data (conventional data matrix) were undertaken by the National Aeronautics and Space Administration (NASA) (Refs. 1 and 2). The NASA investigation, using the six-degree-of-freedom equations of motion, did not result in a good representation of the departure and spin entry flight motions. The results did show that yawing moments produced at high angles of attack were nonlinear with respect to the rotation rate of the airplane. Simulated flight motions using measured large angle static aerodynamics did produce more representative motions in the stall region (Ref. 3).

Because of the apparent inability to realistically simulate spin motions using the conventional aerodynamic data, NASA Langley began a program to measure aerodynamic data on airplane models under constant rotating conditions. This program resulted in the development of a rotation-balance apparatus. The resulting data, measured at steady rotating conditions, were used initially for spin tunnel test correlations (Ref. 4). Additional data obtained from a similar rotation-balance apparatus (Ref. 5) were used in an analytical study of aircraft-developed spin and spin recovery characteristics (Ref. 6). The configurational dependence of the nonlinearities in the aerodynamics, with respect to rotation rate, was demonstrated by the data presented in Refs. 5 and 6.

A refined method for obtaining more accurate rotation-balance aerodynamic data, employing larger models, was developed by NASA. The data obtained from this new technique have been used to analytically simulate representative spinning motions of a 1/10-scale radio-controlled airplane model (Refs. 7 and 8).

The objective of the work presented in this report is to investigate the usefulness of rotation-balance wind tunnel data in computer simulation of full-scale airplane spinning motion. The investigation uses a nonlinear six-degree-of-freedom digital computer program with aerodynamic, inertial, and thrust data for the F-4 series fighter aircraft. Simulated spins are generated utilizing (1) static and forced-oscillation data, and (2) static, forced-oscillation, and rotation-balance data. These simulated spins are in turn compared with time histories of F-4E flight test spins. Specifically, the discussion and evaluation of the application of rotation-balance data in airplane motion simulation will be limited to the steady, flat spin.

2.0 ANALYSIS

2.1 DESCRIPTION OF AIRPLANE

The selection of an airplane configuration to be used in this investigation was influenced by several factors. A current fighter airplane configuration for which high angle-of-attack wind tunnel data were available was desired. Specifically, a comprehensive aerodynamic data matrix including static, forced-oscillation, and rotation-balance data was deemed necessary. In addition, flight test documentation of the basic spin modes and availability of these data were required. Recent wind tunnel tests conducted at Langley Research Center produced a large amount of measured high angle-of-attack aerodynamic data on the F-4 configuration which was documented in Refs. 9 and 10. The Air Force has also conducted extensive full-scale flight tests investigating the stall, departure, and spin characteristics of the F-4E configuration. On the basis of the vast amount of aerodynamic data and flight test results available, the F-4 configuration was selected for this investigation.

A three-view sketch of the general F-4 series airplane configuration is shown in Fig. 1. The mass, inertial, and geometric characteristics used in this investigation are listed in Table 1. These characteristics are for a clean airplane with no external stores other than sparrow missiles at weapon stations 4 and 6. The F-4E characteristics were chosen in order to be consistent with the flight test.

2.2 AERODYNAMIC DATA

The major part of any analytical investigation which calculates the steady-state spin motion of an airplane lies in defining the aerodynamic model to be used. The present study utilizes three types of measured force and moment aerodynamic data: conventional static, forced-oscillation dynamic, and rotation-balance.

All aerodynamic data used in this investigation were compiled from tests conducted in the Langley full-scale tunnel at a speed of approximately 100 ft/sec (Mach No. $\approx$ 0.1), which corresponds to a Reynolds number of about 1.35×10^6 based on wing mean aerodynamic chord. Linear interpolation was used on all aerodynamic table data, unless otherwise noted.

Conventional Data Matrix - The usual method for representing the aerodynamic characteristics of an airplane is a combination of static and forced-oscillation wind tunnel data. The static data used were obtained from Ref. 9 and included the following coefficients:

$$C_x(\alpha, \beta, \delta_H) \; ; \; C_z(\alpha, \beta, \delta_H) \; ; \; C_m(\alpha, \beta, \delta_H)$$

$$C_y(\alpha, \beta, \delta_a) \; ; \; C_\ell(\alpha, \beta, \delta_a) \; ; \; C_n(\alpha, \beta, \delta_a)$$

$$C_y(\alpha, \beta, \delta_r) \; ; \; C_\ell(\alpha, \beta, \delta_r) \; ; \; C_n(\alpha, \beta, \delta_r)$$

These coefficients were measured at angles of attack from -10 to 110 deg in increments of 5 deg and sideslip angles of 0, ±5, ±10, ±15, ±20, ±30, and ±40 deg.

The forced-oscillation derivatives were obtained from Ref. 10 and included the following damping parameters:

$$C_{m_q} - C_{m_{\dot\alpha}} \; ; \; C_{y_p} - C_{y_{\dot\beta}} \sin\alpha \; ; \; C_{y_r} - C_{y_{\dot\beta}} \cos\alpha$$

$$C_{z_q} + C_{z_{\dot\alpha}} \; ; \; C_{n_p} + C_{n_{\dot\beta}} \sin\alpha \; ; \; C_{n_r} - C_{n_{\dot\beta}} \cos\alpha \; ;$$

$$C_{x_q} + C_{x_{\dot\alpha}} \; ; \; C_{\ell_p} + C_{\ell_{\dot\beta}} \sin\alpha \; ; \; C_{\ell_r} - C_{\ell_{\dot\beta}} \cos\alpha \, .$$

It should be noted that the measured coefficients contain terms in $\dot{\alpha}$ and $\dot{\beta}$ which arise from the forced-oscillation measuring technique. For this investigation, these terms are assumed to be zero, as is conventionally done, and the measured damping terms are used as pure derivatives in p, q, and r rates.

These forced-oscillation coefficients were measured at frequencies of 0.7, 1.0, and 1.3 cycles per second and amplitudes of ±5 and ±10 deg over an angle-of-attack range from -10 to 110 deg at 5-deg increments. Also, the "r" derivatives were measured with elevator deflections of 0 and -21 deg for the three frequencies at an amplitude ratio of ±5 deg over the angle-of-attack range. Only the data corresponding to the reduced frequency parameter, K(Ω b/2V or Ω C/2V), obtained from an analysis of the F-4 spins (Ref. 11) and from the static wind tunnel data (Ref. 9) using a first-order approximation [($\omega_{sp} = f(C_{m_\alpha}/I_y)$, $\omega = f(C_{n_\beta}/I_z)$] were incorporated into the simulation data matrix. The longitudinal and lateral/directional damping characteristics incorporated were for a frequency of 0.7 cycles per second and an amplitude of ±5 deg.

Rotation-Balance Data Matrix - The rotation-balance wind tunnel data were obtained with the wind tunnel velocity vector coincident with the airplane model rotation vector. A sketch of the rotation-balance test apparatus used in the full-scale wind tunnel at NASA Langley is shown in Fig. 2. The following coefficients were measured with the rotation-balance apparatus: C_x, C_z, C_m, C_ℓ, C_n, and C_y.

These total coefficients were measured at nondimensional rotation rates (Ωb/2V) of 0, ±0.049, ±0.098, ±0.196, ±0.245, and ±0.294, pitch angles of 55 to 90 deg in 5-deg increments, and bank angles of 0, 5, and 10 deg. The tunnel roll and pitch angles are related to the airplane angle of attack and sideslip by

$$\alpha = \tan^{-1} (\tan \theta \cos \phi)$$

$$\beta = \sin^{-1} (\sin \theta \sin \phi)$$

The incremental rotation-balance data used in this investigation included data measured with all controls neutral, elevator control at -21 deg, and with left and right pro-spin controls deflected (left: δ_H = -21 deg, δ_a = -30 deg, δ_r = 30 deg; right: δ_H = -21 deg, δ_a = 30 deg, δ_r = -30 deg). To represent the aerodynamic damping effect of oscillations superimposed on a steady rotation, forced-oscillation derivatives were used with the rotation-balance data.

Significant magnitudes of rotation rate are known to develop in fighter airplane stall/post-stall gyrations below 55 deg angle of attack. The incremental rotation-balance data effects at 55 deg angle of attack were extrapolated to 30 deg angle of attack for possible excursions in this region due to control perturbations.

2.3 METHOD OF ANALYSIS

Airplane steady-state spins are generally characterized by sustained turning motion at a stalled angle of attack. To adequately represent these motions in an analytical investigation requires the complete six-degree-of-freedom equations of motion. A comprehensive matrix of measured nonlinear aerodynamic data are also required for these high angle-of-attack flight regions. The following discussion describes the equations of motion and the aerodynamic data models used in the investigation.

The differential equations of motion are presented in Appendix A (see A.1). Also presented are equations defining parameters required by the six-degree-of-freedom equations. The method by which the aerodynamic force and moment data were combined to evaluate the inclusion of rotation-balance data in spin simulation will now be described. (Further discussion may be found in Appendix B.) Three aerodynamic models were formulated from the previously described force and moment data. Aero Model 1 represents the conventional technique which does not include the aerodynamic forces and moments acting on the spinning airplane because of steady rotational flow and does not restrict the dynamic oscillatory derivatives to the oscillatory component of the total angular rates. Aero Model 2 represents the conventional technique in which the dynamic oscillatory derivatives are restricted to the oscillatory component of the total angular rates. Aero Model 3 represents the aerodynamic model based on the rotation-balance data in which the dynamic oscillatory and rotation-balance data are restricted to the oscillatory and steady rotation components of the total angular rates, respectively.

The initial conditions and control deflections used in the analytical simulations were obtained from Ref. 11 and are documented in Table 2. These initial conditions, along with the mass and inertia characteristics and each of the aerodynamic models, were input into the computer program. The program was numerically intergrated with time by using a fourth-order Runge-Kutta integration algorithm with a fixed integration stepsize (Ref. 12). An examination of the computed motions for each aerodynamic model then indicated the success of the simulation attempt.

3.0 RESULTS AND DISCUSSION

The simulation of a steady, flat spin was performed using the three aerodynamic data models described in Section 2.3. A flight test spin characterized as a flat spin was selected as a correlation base because of the proximity of the velocity and spin rate vectors. The relationship of the velocity and spin vectors of the chosen spin more closely agreed with the conditions under which the rotation-balance wind tunnel data were obtained. This particular spin, although characterized as a flat spin, was accompanied by small oscillations in all rates and angles. These oscillations were repetitive, with amplitudes of less than ±20.0. The initial conditions used in the simulation were obtained from a time history presented in Ref. 11 documenting the F-4E stall/near-stall characteristics. The necessary parameters required for the simulation were extracted from these time histories at a time the spin was considered to be in a steady, flat mode. This time was selected at 85 sec into the spin.

Flight motions calculated using measured static and forced-oscillation aerodynamic data (Aero Model 1) are shown in comparison with the flight test motion in Fig. 3. The technique used in extracting the flight test components is presented in Appendix C. It should be noted here that the symbols presented for the calculated characteristics are cosmetic, whereas the solid line represents the actual calculated points. As can be seen in this figure, the calculated motions generated require approximately 40 sec to stabilize. The motions beyond 40 sec can be considered representative of the flight test spin characteristics. The perturbations in the calculated motions during the first 40 sec can be attributed to the lack of balance between the aerodynamic, inertia, and thrust contributions in the moment equations of motion. The unsteadiness can be seen in Fig. 3, where the aerodynamic contributions $\dot{p}_{AERO}$, $\dot{q}_{AERO}$, and $\dot{r}_{AERO}$ to the total moment equations of motion are presented along with flight test data.

Flight motions calculated using measured static and forced-oscillation aerodynamic data, in which the forced-oscillation derivatives were restricted to the oscillatory components of the total angular rates (Aero Model 2), are shown in Fig. 4. The flight motions are also shown for comparison. The overall spin characteristics are changed by Aero Model 2 and result in a gradual reduction in angle of attack and total angular rate (Ω) with time. The motion is suppressed to a nonoscillatory state which is not characteristic of the flight test spin. The suppression of $\dot{p}_{AERO}$, $\dot{q}_{AERO}$, and $\dot{r}_{AERO}$ to a nonoscillatory state strongly indicates the importance of including the influence of steady rotation on the aerodynamics.

Flight motions were calculated by incorporating the rotation-balance aerodynamic data (Aero Model 3). A comparison of the calculated and flight test motions is shown in

Fig. 5. Although the attitude angles and rotation rates of the calculated motions are not exact overlays of the flight test motions, these results are considered quite representative since completely unaltered aerodynamic data were used. A brief examination of the time history reveals that the aerodynamic modeling as shown by the calculated terms $\dot{p}_{AERO}$, $\dot{q}_{AERO}$, and $\dot{r}_{AERO}$ more closely duplicates the flight characteristics than either Aero Model 1 or 2. Some discrepancy in the longitudinal aerodynamic model is indicated by the lack of correlation between the calculated and flight test values of $\dot{q}_{AERO}$.

The general conclusions previously drawn indicate that for the specific flight test motions simulated, use of either Aero Model 1 or 3 would yield representative spin motions. This general conclusion resulted in an attempt to answer the question whether representative spin motions could be obtained using Aero Models 1 and 3 for other initial conditions. The thought here was to introduce a change in the initial conditions that would yield a known result. This led to the application of left pro-spin controls (LPSC) at the start of the calculated motion. In general, application of pro-spin controls should result in an increase in the spin rate and angle of attack with some reduction in the oscillatory characteristics.

Figure 6 presents a comparison of the calculated motions using Aero Models 1 and 3 for application of LPSC. For Aero Model 1, the application of LPSC resulted in driving the simulated airplane out of the spin. This result can be explained by the control power characteristics in the 50- to 65-deg angle-of-attack range; both rudder and aileron produce a retarding moment in this angle-of-attack range. The initial perturbations resulting from application of LPSC drives the calculated motion into this angle-of-attack region. Application of LPSC to Aero Model 3 increased the spin rate. This influence resulted in a gradual suppression of the oscillatory characteristics along with an increase in angle of attack and spin rate (Ω). The resultant motions for Aero Model 3 were as expected for application of pro-spin controls, whereas for Aero Model 1 they were not. Application of pro-spin controls to Aero Model 3 improved the correlation with the flight test spin. This improvement in the flight correlation resulting from application of LPSC indicates possible discrepancies in the static aerodynamic model.

An attempt was made to simulate the steady, flat spin using Aero Model 3 without the forced-oscillation derivatives. A comparison of the calculated motions with and without forced-oscillation derivatives is shown in Fig. 7. The calculated motions without forced-oscillation derivatives were terminated at 8 sec because of the oscillatory divergence that resulted in exceeding the aerodynamic data range in sideslip. This result indicates the necessity of including some type of damping data to handle oscillations in p and q. Oscillatory damping data for both pitch and roll could not be obtained by the technique used in acquiring the steady-state rotation-balance data.

Further investigation was made to determine which of the incremental moment contributions ($\Delta C_{\ell_{rb}}$, $\Delta C_{m_{rb}}$, or $\Delta C_{n_{rb}}$) caused by steady-state rotation were most important in maintaining the steady spin. Figures 8, 9, and 10 present the results obtained for steady spin attempts using Aero Model 3 when these moment contributions are implemented separately. The calculated motion, which includes all force and moment contributions caused by steady rotation, shown earlier in Fig. 5, is presented in Figs. 8, 9, and 10 for comparison. An examination of Figs. 8 and 10 reveals that the results for individual implementation of the rolling and yawing moment contributions ($\Delta C_{\ell_{rb}}$ and $\Delta C_{n_{rb}}$) caused by steady rotation are quite representative of those including all rotation-balance data. In general, the oscillatory characteristics are slightly more suppressed for the inclusion of $\Delta C_{n_{rb}}$ than for $\Delta C_{\ell_{rb}}$ alone. The calculated motions using Aero Model 3 for $\Delta C_{m_{rb}}$ alone result in a gradual reduction in angle of attack and total angular rate (Ω). The motion is suppressed to a nonoscillatory state which is not representative of the calculated motions, including all rotation-balance data as well as the flight test spin. A comparison of the calculated motions presented in Figs. 4 and 9 confirms that the pitching-moment contribution caused by steady rotation, $\Delta C_{m_{rb}}$, alone has little influence on the calculated motions. For this configuration, the most significant factor that must be included in the aerodynamic model for steady spin calculation is the nonlinear variation of the rolling- and yawing-moment contributions caused by rotation rate.

Once it was established that the rotation-balance data system (Aero Model 3) was best for calculating the steady, flat spin for the test configuration, an attempt was made to determine possible sources of error preventing better calculated/flight test correlation. Previous conclusions indicated that the most obvious discrepancy was in the longitudinal aerodynamic model. This is better pointed out by the lack of correlation between the calculated and flight test values of $\dot{q}_{AERO}$ shown in Fig. 5. The incremental difference between mean values of flight test and calculated $\dot{q}_{AERO}$ corresponds to an increment in pitching moment between 0.12 and 0.17.

Results from the application of LPSC in the calculated motions indicated possible discrepancies in the static aerodynamic data. Therefore, additional static longitudinal wind tunnel data (normal-force and pitching-moment data) were obtained from a 1/15-scale model F-4D test at NASA Ames (Ref. 13). The NASA Langley data used in the previously calculcated motions are presented along with the NASA Ames data in Figs. 11 and 12 for comparison. The NASA Ames test was conducted at a Reynolds number of 4.0×10^6 per foot, whereas the Langley test was conducted at a Reynolds number of 1.35×10^6 per foot. Assuming that the differences between the Ames and Langley data are not caused by model configuration, the difference in the normal-force and

pitching-moment data at angles of attack above approximately 20 deg (stall) is most probably caused by Reynolds number and/or sting/support interference, as indicated in Ref. 14. A comparison of the incremental differences between the Ames and Langley data in the stall angle-of-attack region gives credence to the possibility of Reynolds number effects. In the higher Reynolds number test, an increase in lift occurs with a resulting reduction in pitching moment. In the spin angle-of-attack region (α = 55 to 75 deg), the increments in normal force and pitching moment vary between -0.10 and -0.15 for ΔC_z and between 0.125 and 0.175 for ΔC_m. Somewhat of a surprise is the fact that the incremental difference betwen the mean values of flight test and calculated aerodynamic pitching moment (Fig. 5) corresponds to the increments between the Ames and Langley data (Fig. 12). It should be noted that the average Reynolds number for the flight test spin was 14.0 x 10^6.

Calculations were made to determine the effects on the steady spin motion of these increments in static normal force and pitching moment. Spin motions were calculated using Aero Model 3 and the minimum and maximum values of the increments in C_z and C_m between the Langley and Ames data. Figure 13 presents a comparison of the spin calculations for the minimum and maximum values of the increments in C_z and C_m between the Langley and Ames data. The overall results for the calculated spins for each set of increments are not significantly different. Figure 14 presents a comparison of calculated spins for Aero Model 3 and Aero Model 3 with increments in ΔC_z of -0.15 and in ΔC_m of 0.175. The flight test motion is also shown in Fig. 14 as a means of determining whether any improvements in correlation were made. The results obtained for increments of ΔC_z = -0.15 and ΔC_m = 0.175 significantly improve the flight test correlation and strengthen the basis for requiring model data corrected for such effects as Reynolds number, sting and wall interference, and model configuration differences.

The above results indicate that a good static data matrix is necessary for better correlation with flight test data, but does not eliminate the predominant oscillatory characteristic in pitch. An attempt at determining the source of error led to a review of the flight test aerodynamic data. In particular, the contributions to the flight pitch angular acceleration due to thrust, aerodynamics, and inertial coupling determined from the time history are shown in Fig. 15. The oscillatory characteristic of flight test $\dot{q}_{TOTAL}$ is dramatically influenced by the inertial coupling component and not by the aerodynamic component. This indicates that the oscillatory characteristic of the calculated $\dot{q}_{AERO}$ as shown in Fig. 14 could be caused by a discrepancy in the forced-oscillation pitch-damping wind tunnel data. In light of this possibility, a review of the forced-oscillation pitch data (solid-line fairing in Fig. 16) used in the calculations revealed a large reduction in (C_{m_q} + $C_{m_{\dot{\alpha}}}$) in the spin angle-of-attack region (α = 55 to

80 deg). However, additional forced-oscillation data (long/short dash fairing) obtained on a 1/11-scale F-4B model at a Reynolds number of 0.45 x 10^6 per foot did not exhibit the same trend in the spin angle-of-attack region; a comparison of the 1/11-scale data with that used for the calculated motion is shown in Fig. 16. The agreement in the data up to approximately stall angle of attack ($\alpha \approx 23$ deg) indicates that differences in the stall/spin angle-of-attack region are not caused by model configuration but possibly are caused by Reynolds number, sting, and wall interference effects. The incremental differences in the stalled angle-of-attack region are characteristics of Reynolds number effect. Since the 0.13-scale data were obtained at a higher Reynolds number, they were retained and modified as indicated by the dashed-line fairing in the 55- to 80-deg angle-of-attack region.

Figure 17 presents a comparison of the time history spin calculations using Aero Model 3 with and without modifications in the static and forced-oscillation pitch data [ΔC_z = -0.10, ΔC_m = 0.125, (C_{m_q} + $C_{m_{\dot{\alpha}}}$) fairing] and the flight test time history. The resultant motions for the modified data more closely model the longitudinal flight characteristics. This is shown in Fig. 17 by the much improved relationship between the calculated and flight test values of α, q, and $\dot{q}_{AERO}$. It should be pointed out that with these modifications, the calculated motion exhibits a slight overdamping in the lateral/directional characteristics. The indications are that possible modifications in the lateral/directional data matrix would be necessary. In general, the overall calculated/flight test correlation is much improved by the data matrix modifications.

4.0 CONCLUDING REMARKS

The results of this analytical investigation of steady spin characteristics of the F-4 series airplane using conventional and rotation-balance aerodynamic data are summarized as follows.

1. For the configuration investigated, the use of conventional static and forced-oscillation aerodynamic data as combined in Aero Models 1 and 2 would not result in maintaining the steady, flat spin motions.

2. The inclusion of rotation-balance data in the aerodynamic data matrix (Aero Model 3) resulted in calculated motions that are considered representative of the flight test steady spin. The inclusion of forced-oscillation data to account for the effects of oscillations in roll and pitch superimposed on the steady spin motion were found to be necessary in order to maintain the steady spin. For this configuration, the most significant factor that must be included in aerodynamic modeling for steady spin simulation is the nonlinear variation of the rolling and yawing moment contributions caused by steady rotation.

3. The major deficiency in utilizing rotation-balance data in this type of simulation is the lack of a complete set of measured data. The rotation-balance data at sideslip angles up to 15 deg were quite adequate for the flight test spin investigated; however, measured rotation-balance data should be obtained at larger angles of sideslip for application in the flight regime between initial stall and steady spins. Rotation-balance data should be obtained down to at least stall angle of attack for attempted simulation of stall/post-stall gyration maneuvers.

REFERENCES

1. Scher, S. H., Anglin, E. L., and Lawrence, G. F. "Analytical Investigation of Effect of Spin Entry Technique on Spin and Recovery Characteristics for a 60° Delta-Wing Airplane." NASA TN D-156, December 1959.

2. Chambers, J. R., Anglin, E. L., and Bowman, J. S., Jr. "Effects of a Pointed Nose on Spin Characteristics of a Fighter Airplane Model Including Correlation with Theoretical Calculations." NASA TN D-5921, September 1970.

3. Moore, F. L., Anglin, E. L., Adams, M. S., Deal, P. L., and Person, L. H., Jr. "Utilization of a Fixed-Base Simulator to Study the Stall and Spin Characteristics of Fighter Airplanes." NASA TN D-6117, March 1971.

4. Bamber, J. J. and House, R. O. "Spinning Characteristics of the XN2Y-1 Airplane Obtained from the Spinning Balance and Compared with Results from the Spinning Tunnel and from Flight Tests." NACA Rep. 607, 1937.

5. Stone, R. W., Jr., Burk, S. M., Jr., and Bihrle, W., Jr. "The Aerodynamic Forces and Moments on a 1/10-Scale Model of a Fighter Airplane in Spinning Attitudes as Measured on a Rotary Balance in the Langley 20-Foot Free-Spinning Tunnel." NACA TN-2181, September 1950.

6. Anglin, E. L. and Scher, S. H. "Analytical Study of Aircraft-Developed Spins and Determination of Moments Required for Satisfactory Spin Recovery." NASA TN D-2181, February 1964.

7. Bihrle, W., Jr. and Barnhart, B. "Effects of Several Factors on Theoretical Predictions of Airplane Spin Characteristics." NASA CR-132521, Grumman Aerospace Corporation, August 1974.

8. Bihrle, W., Jr. "Correlation Study of Theoretical and Experimental Results for Spin Tests of a 1/10-Scale Radio Control Model." NASA CR-144995, Grumman Aerospace Corporation, December 1975.

9. Anglin, Ernie L. "Static Force Tests of a Model of a Twin-Jet Fighter Airplane for Angles of Attack from -10° to 110° and Sideslip Angles from -40° to 40°." NASA TN D-6425, August 1971.

10. Grafton, Sue B., and Libbey, Charles E. "Dynamic Stability Derivatives of a Twin-Jet Fighter Model for Angles of Attack from -10° to 110°." NASA TN D-6091, January 1971.

11. McElroy, Collett and Sharp, Patrick S. "Stall/Near Stall Investigation of the F-4E Aircraft." FTC-SD-70-20, 1970.

12. North American Rockwell. Digital Simulation User's Manual. NR70H-232-2, June 1970.

13. F-4 Spin Evaluation Program, MDC A0005, Volume II, August 1969.

14. Eulrich, B. J. and Weingarten, N. C. "Identification and Correlation of the F-4E Stall/Post-Stall Aerodynamic Stability and Control Characteristics from Existing Test Data." AFFDL-TR-73-125, Calspan Corporation, August 1973.

15. Kroll, W. B. "An Analytical Investigation of the Stall, Departure, and Spin Entry Characteristics of a Current Fighter Airplane Using Conventional and Rotary Aerodynamic Models." Masters Thesis, George Washington University, August 1976.

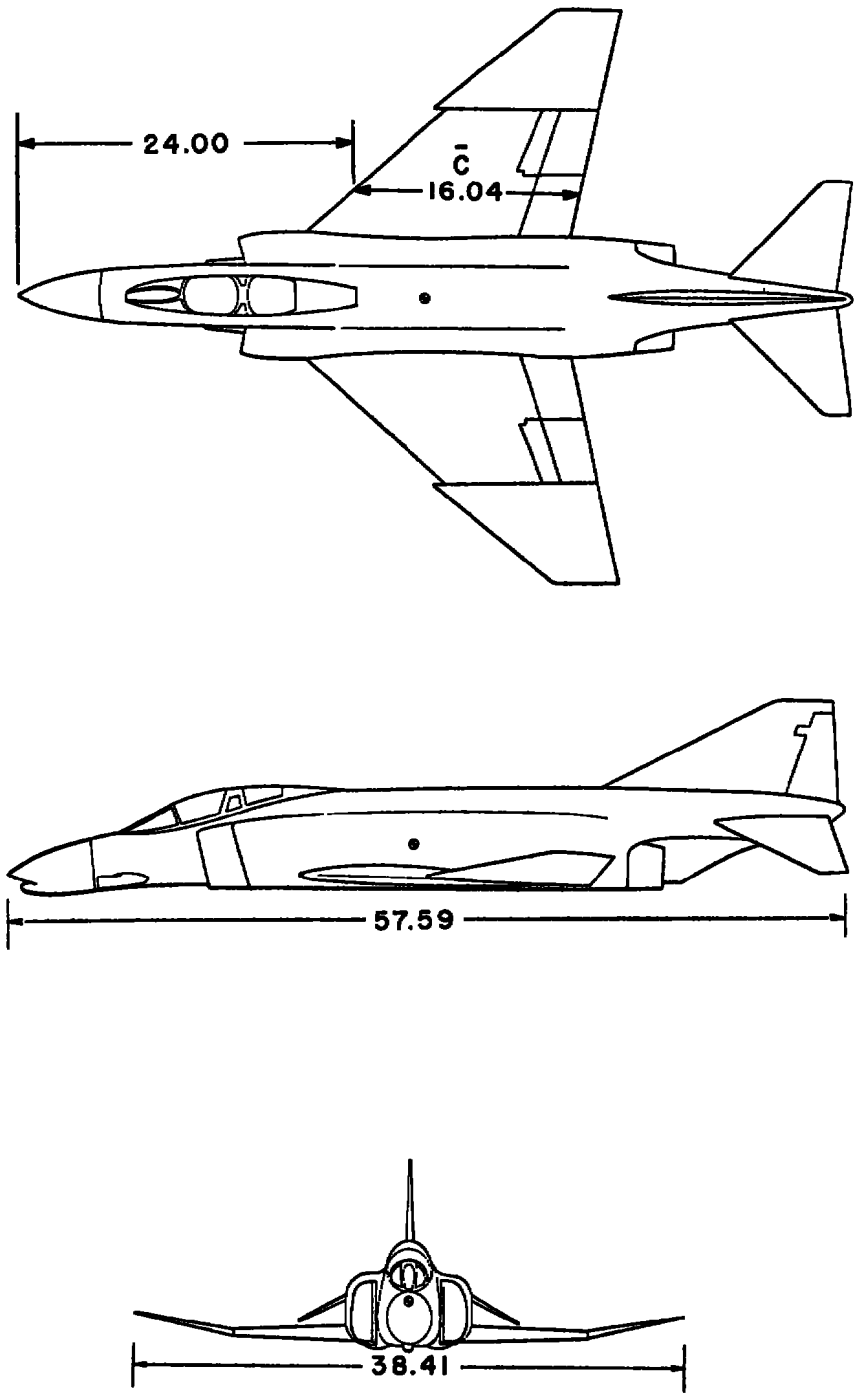

DIMENSIONS IN FEET

Figure 1. Three-view sketch of the F-4 airplane.

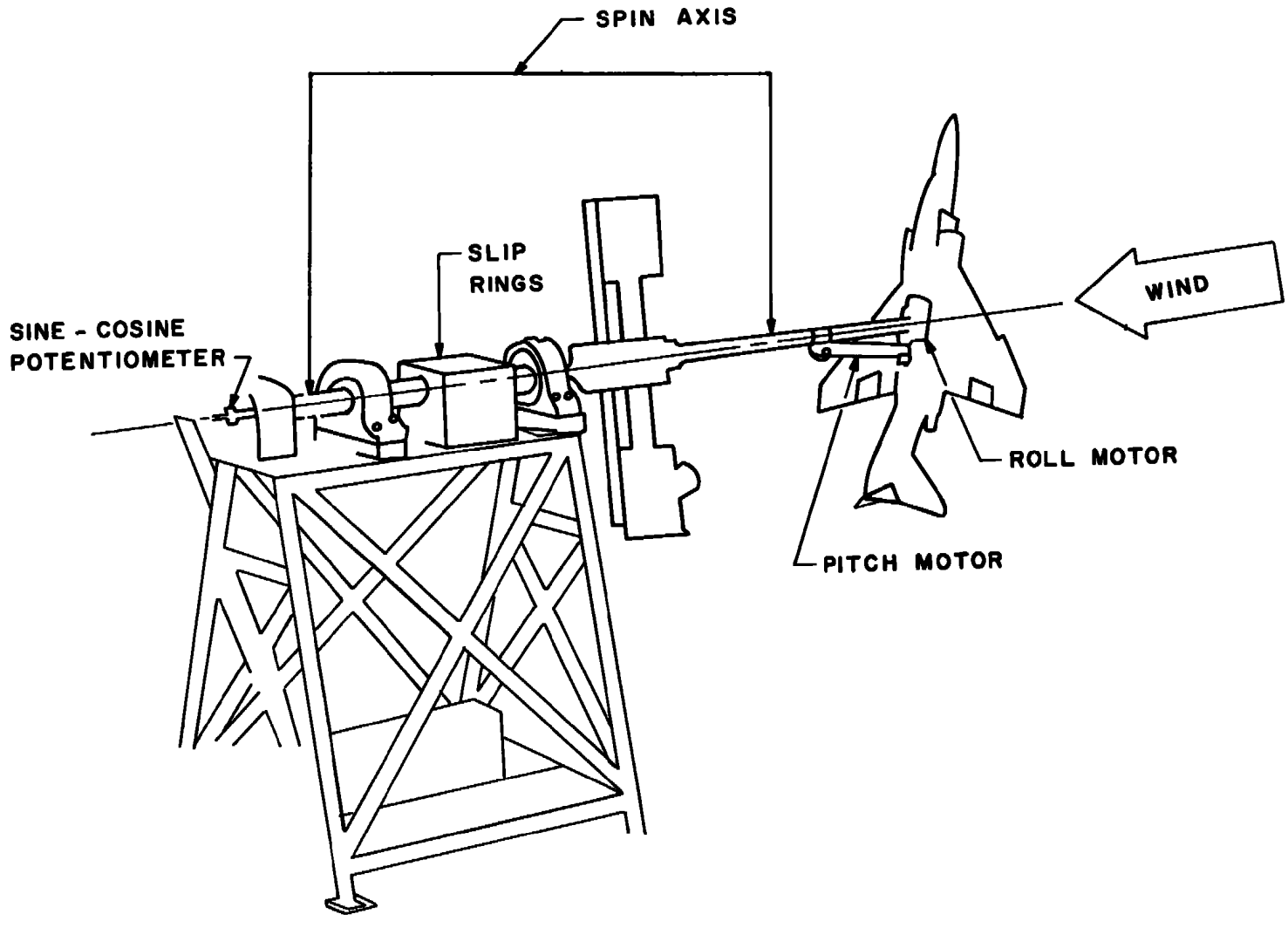

Figure 2. Rotation-balance apparatus.

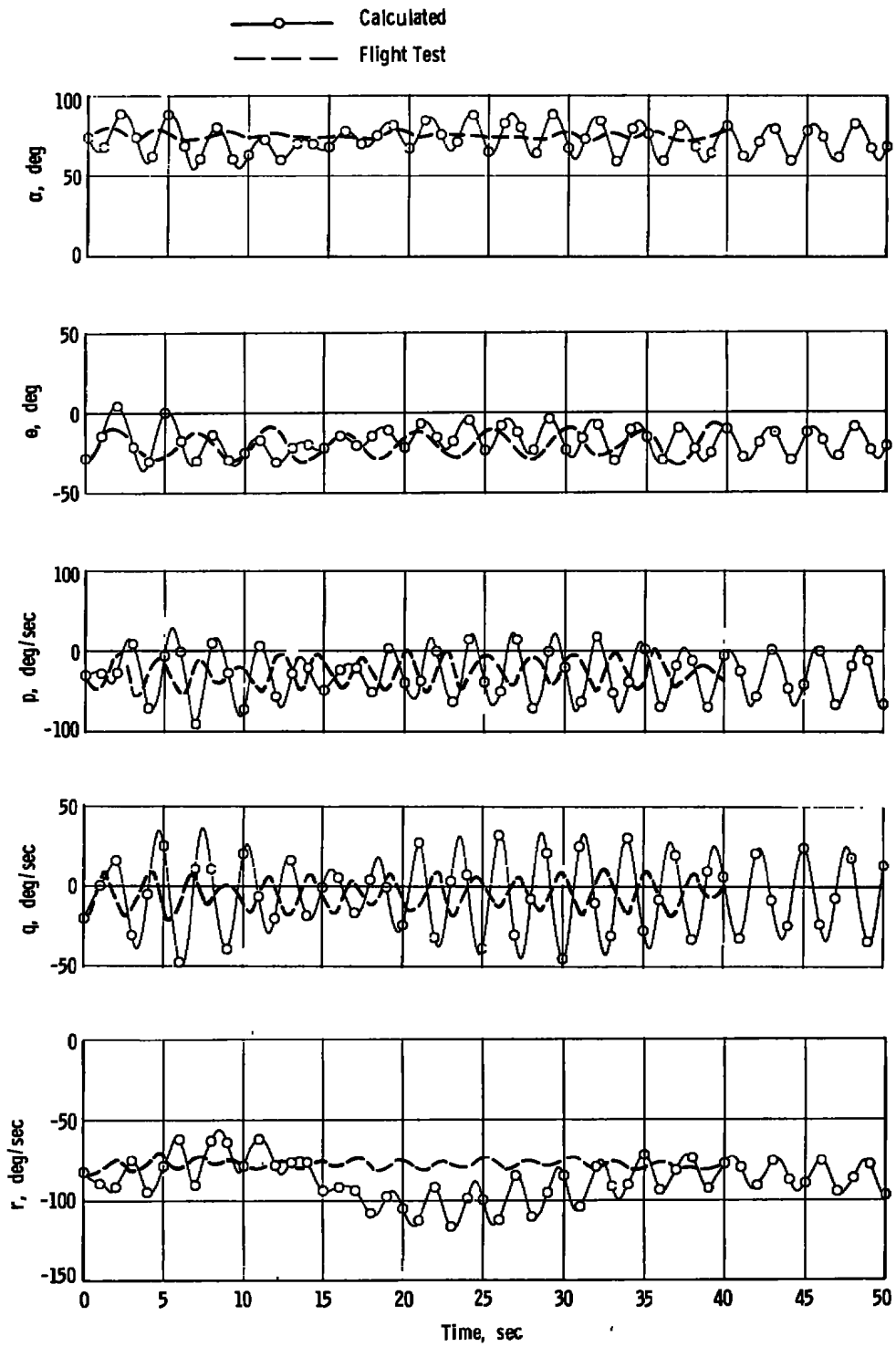

Figure 3. Comparison of calculated motions using Aero Model 1 and airplane flight motions.

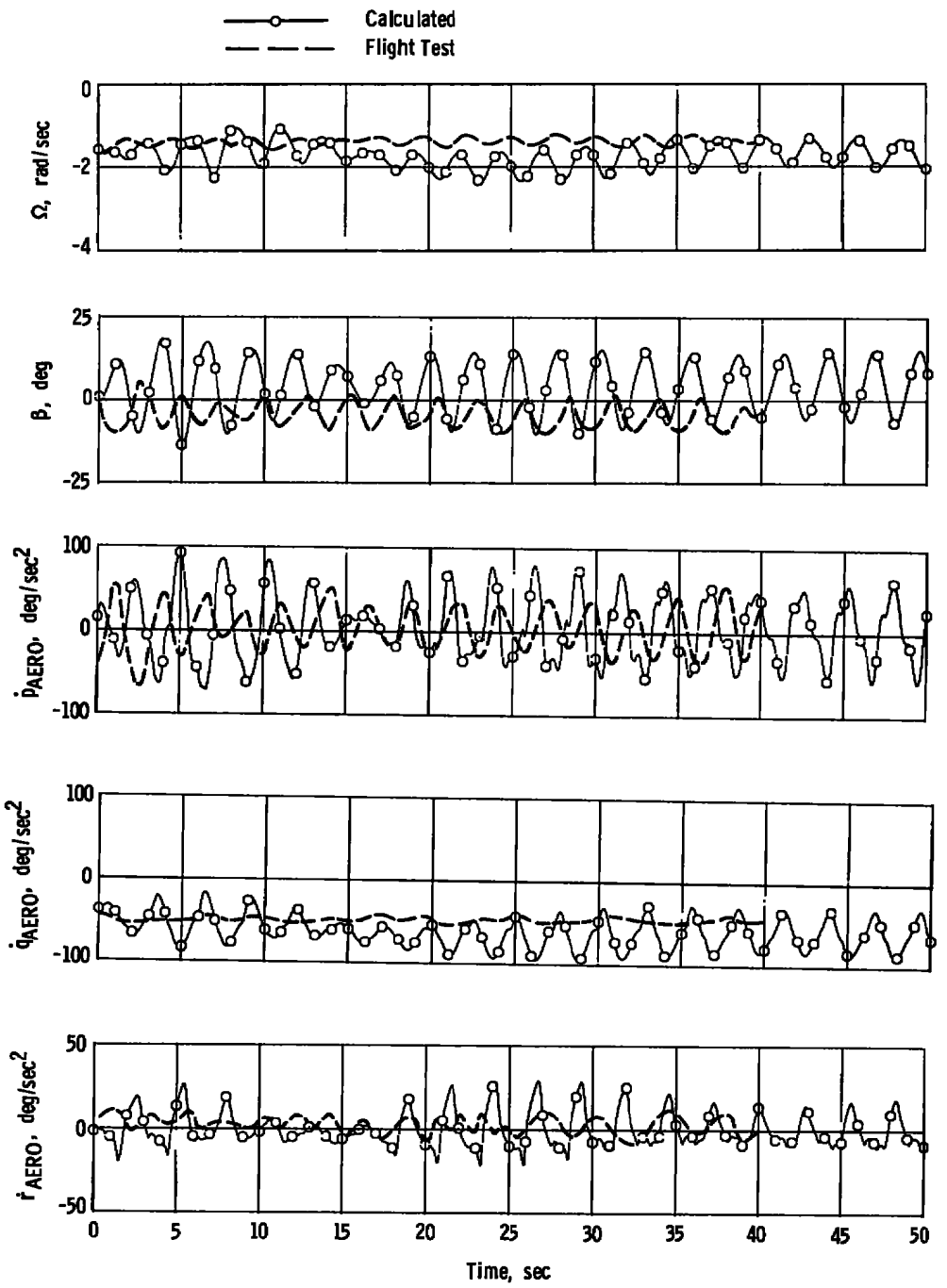

Figure 3. Concluded.

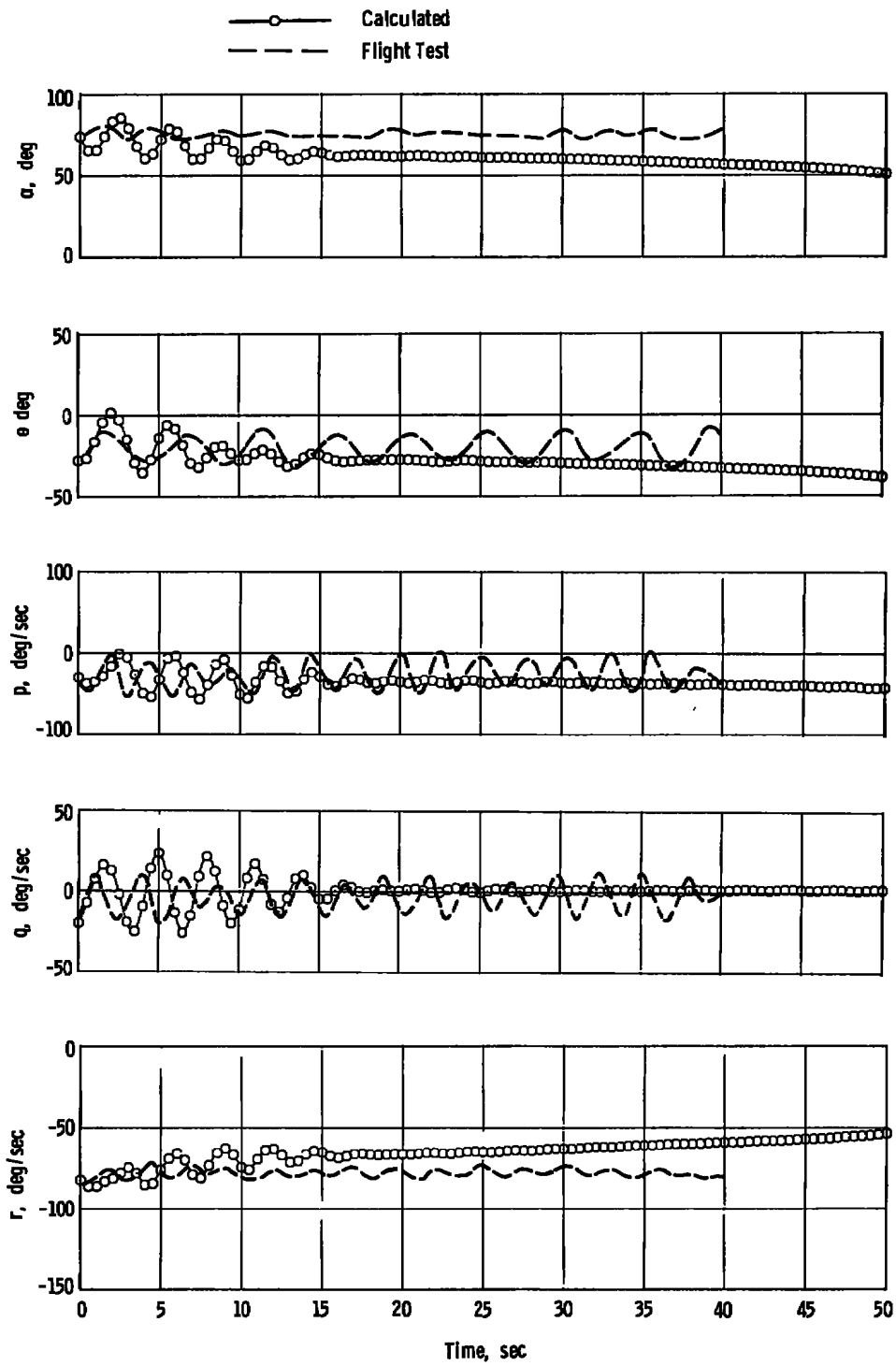

Figure 4. Comparison of calculated motions using Aero Model 2 and airplane flight motions.

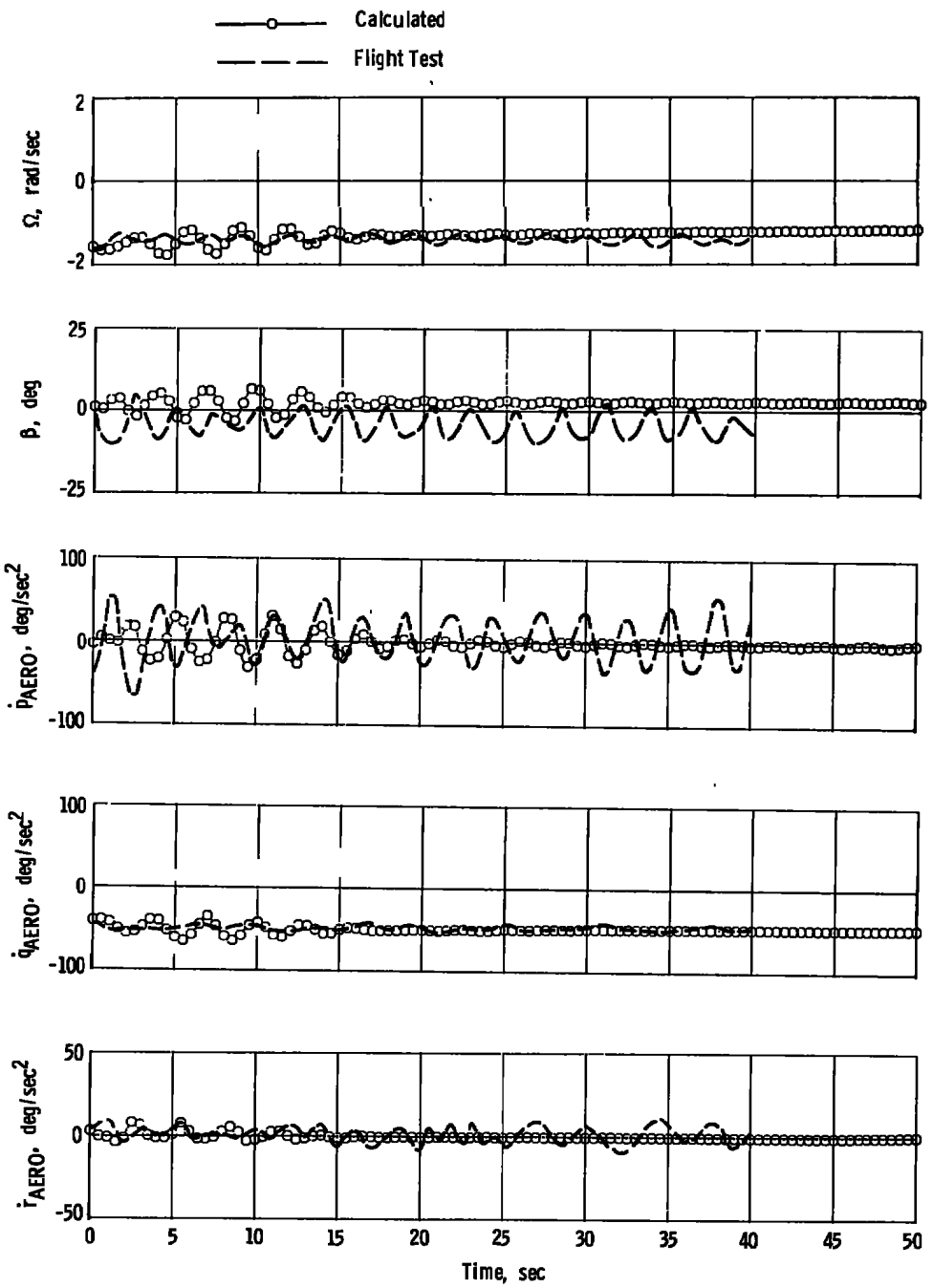

Figure 4. Concluded.

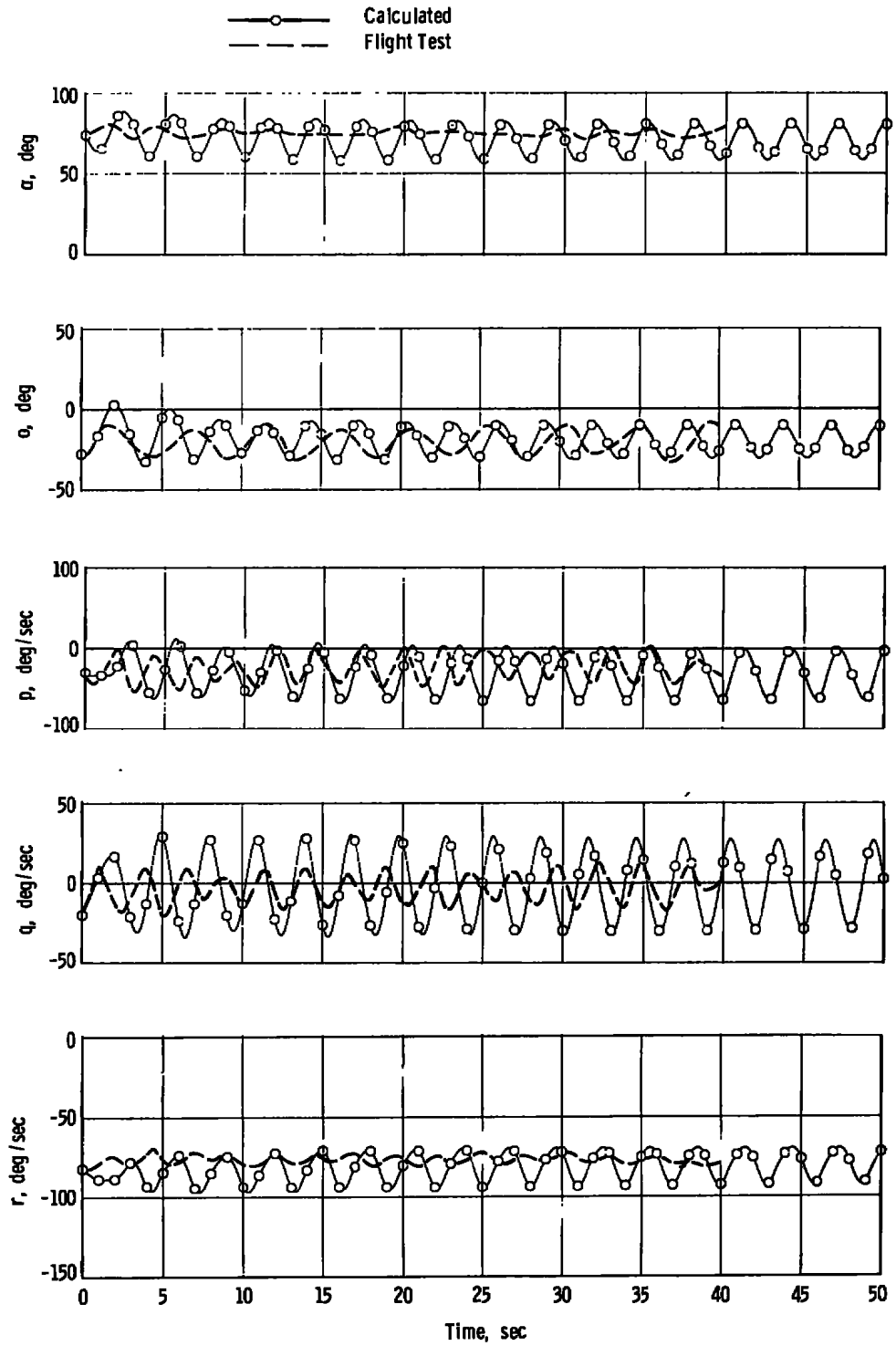

Figure 5. Comparison of calculated motions using Aero Model 3 and airplane flight motions.

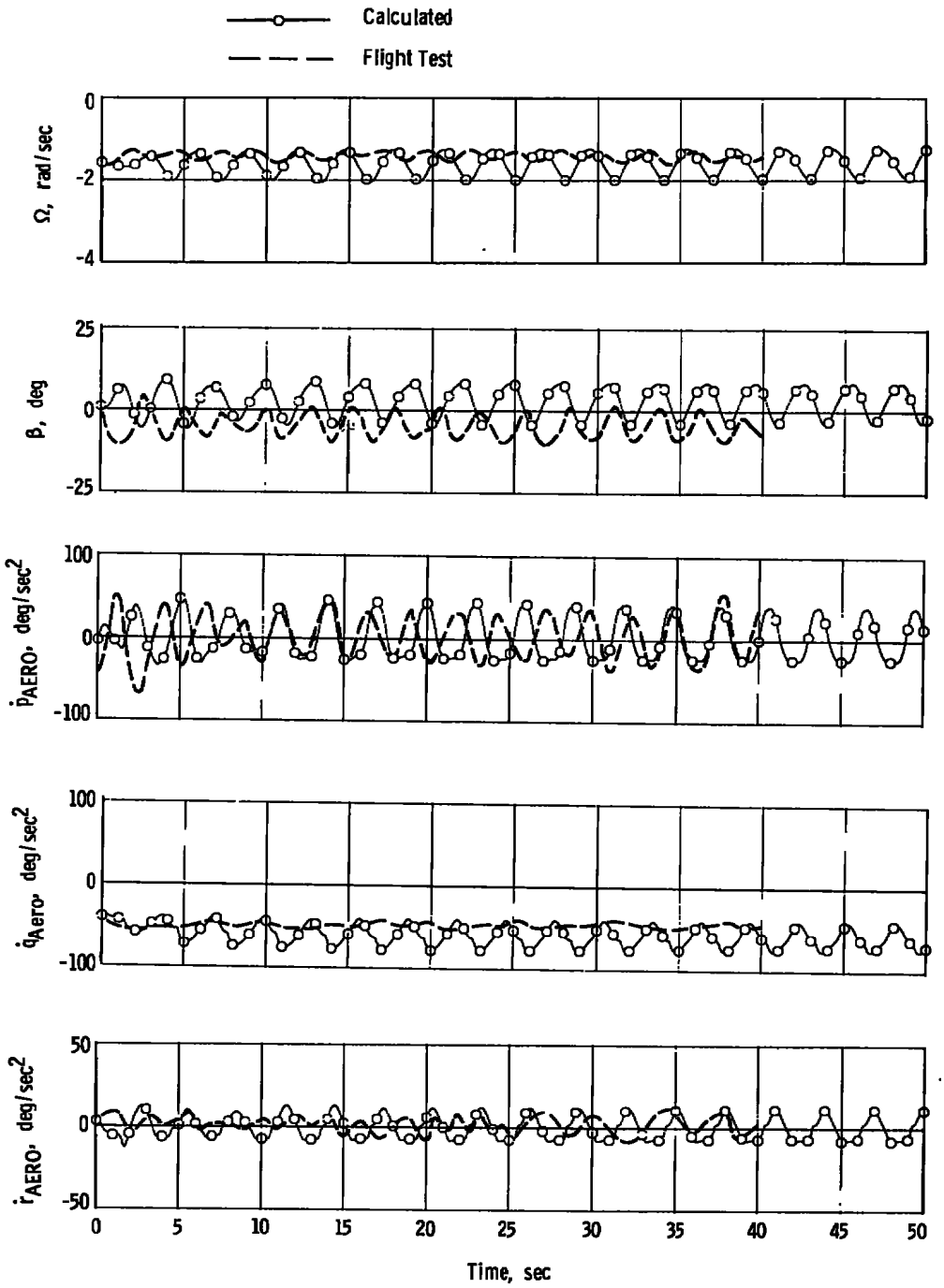

Figure 5. Concluded.

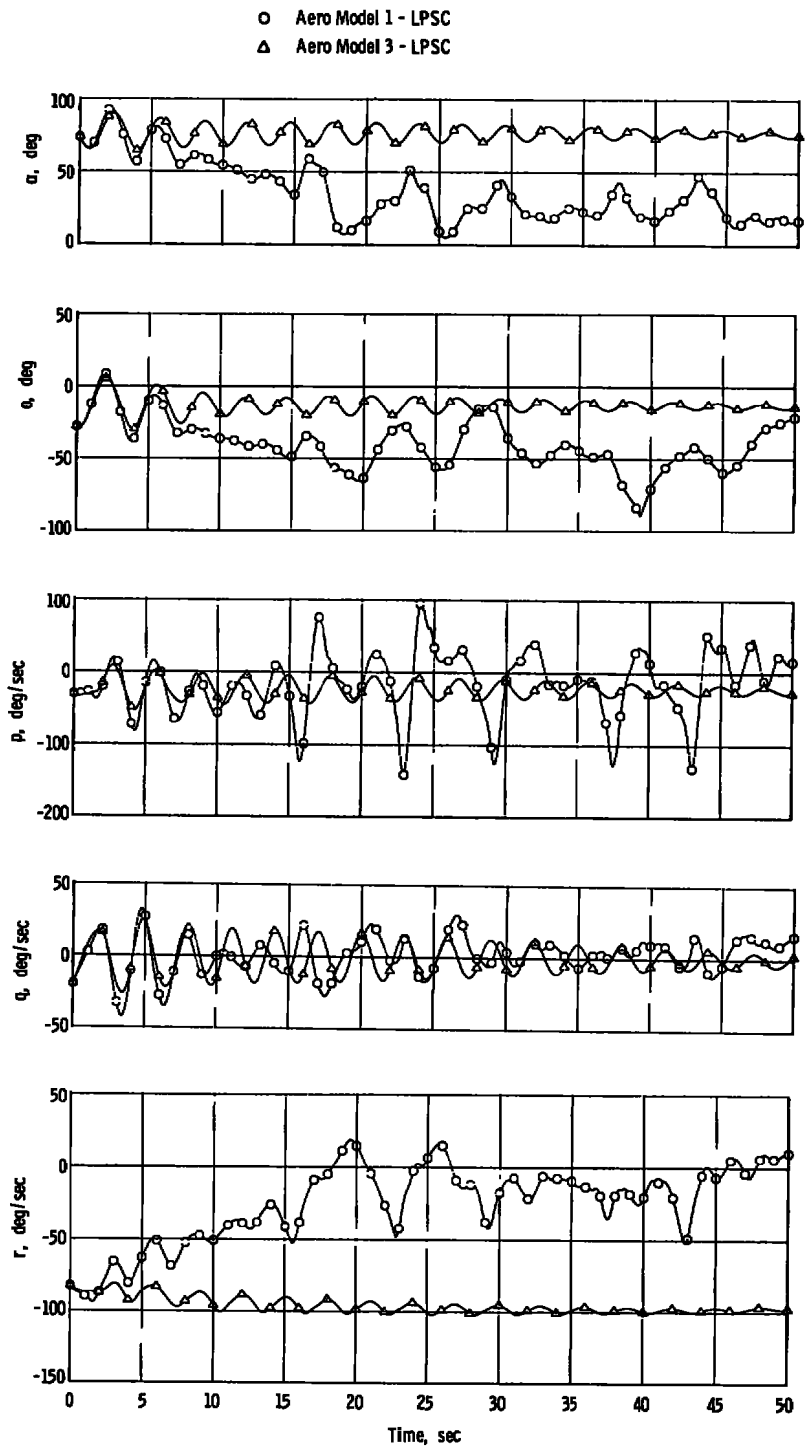

Figure 6. Comparison of calculated motions for Aero Models 1 and 3, left pro-spin controls.

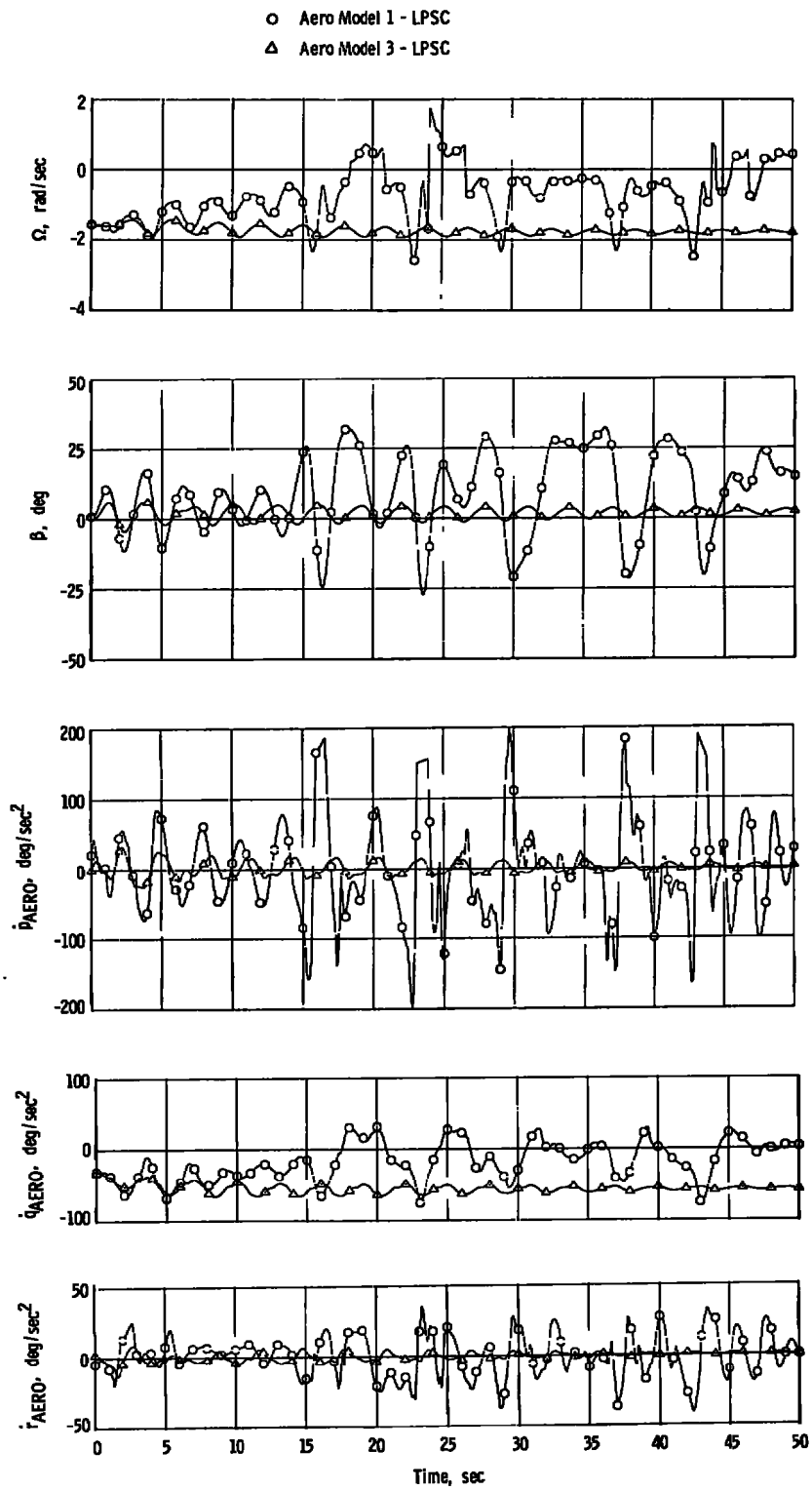

Figure 6. Concluded.

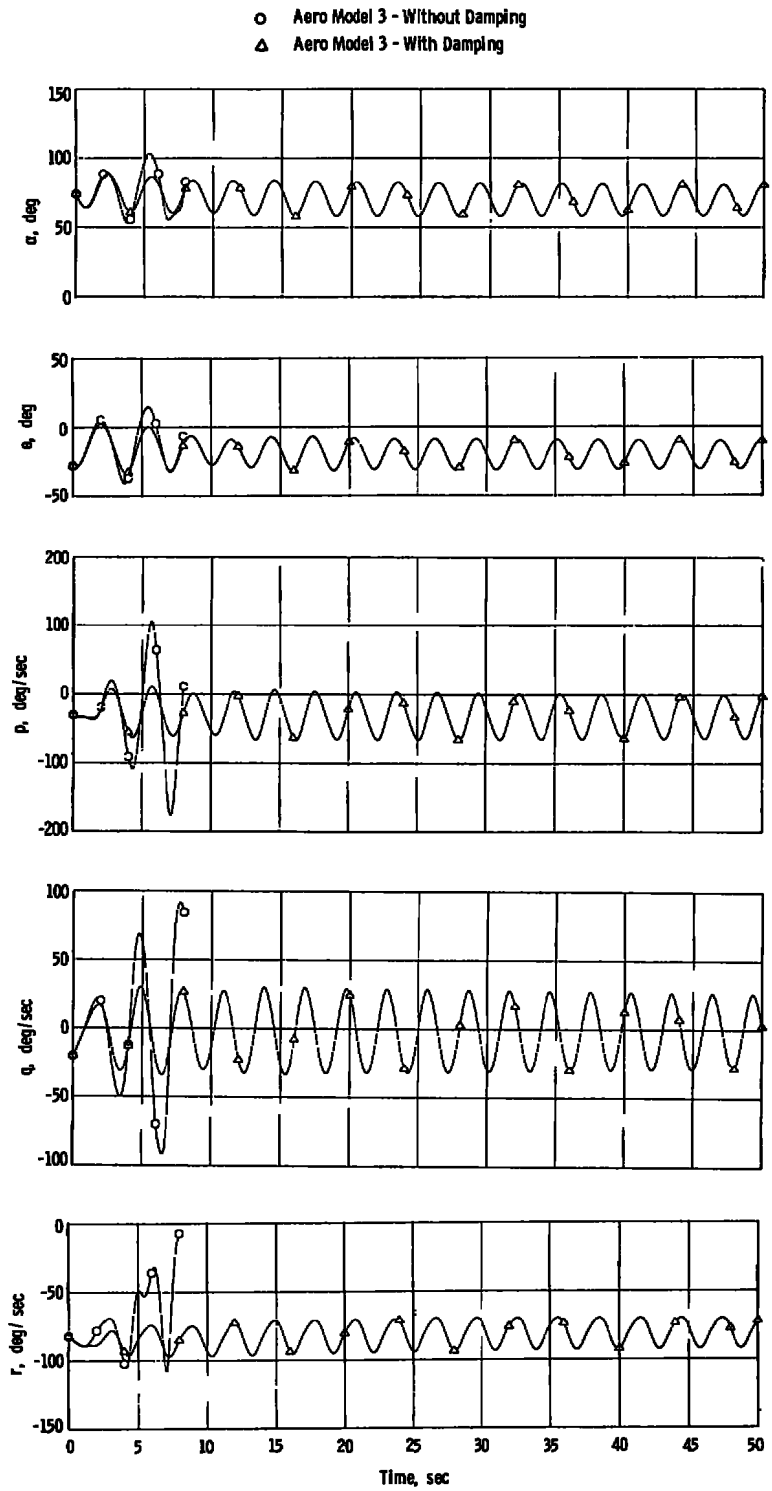

Figure 7. Comparison of calculated motions using Aero Model 3 with and without forced-oscillation damping data.

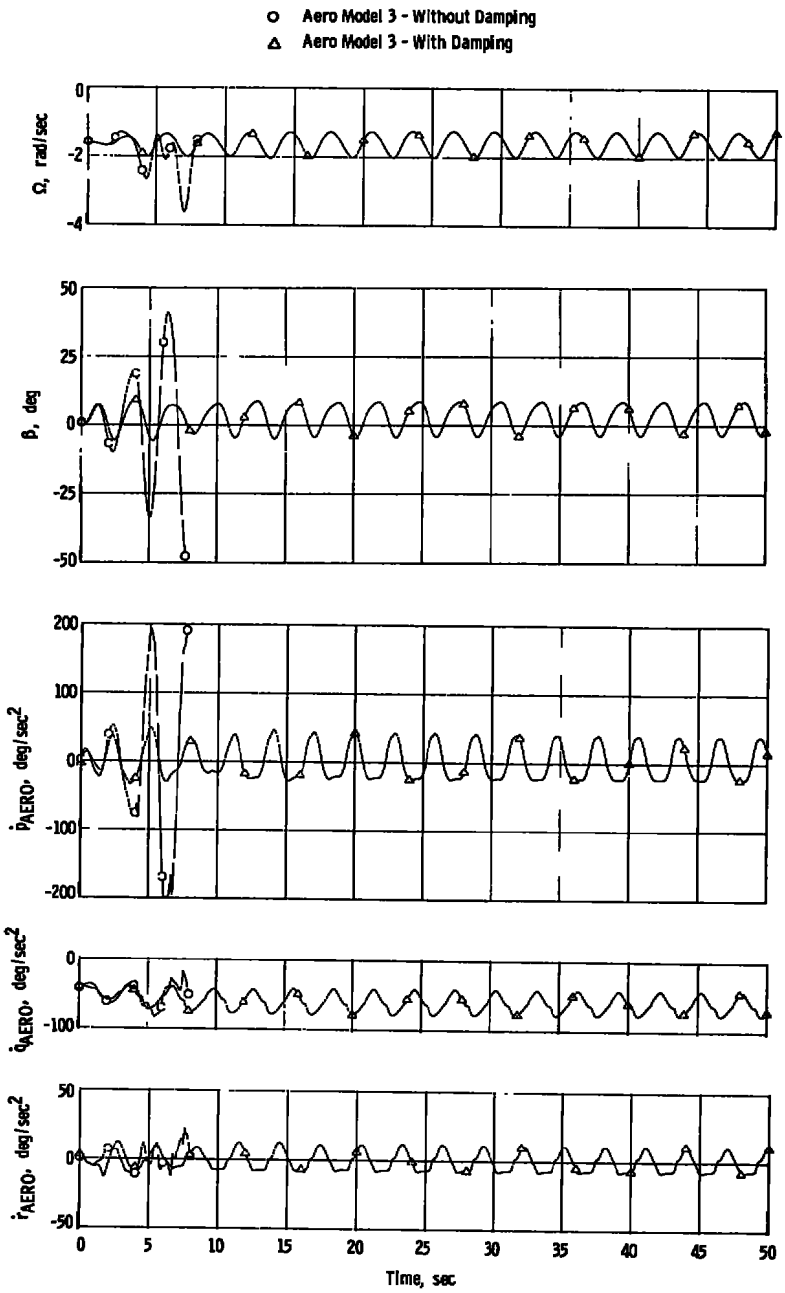

Figure 7. Concluded.

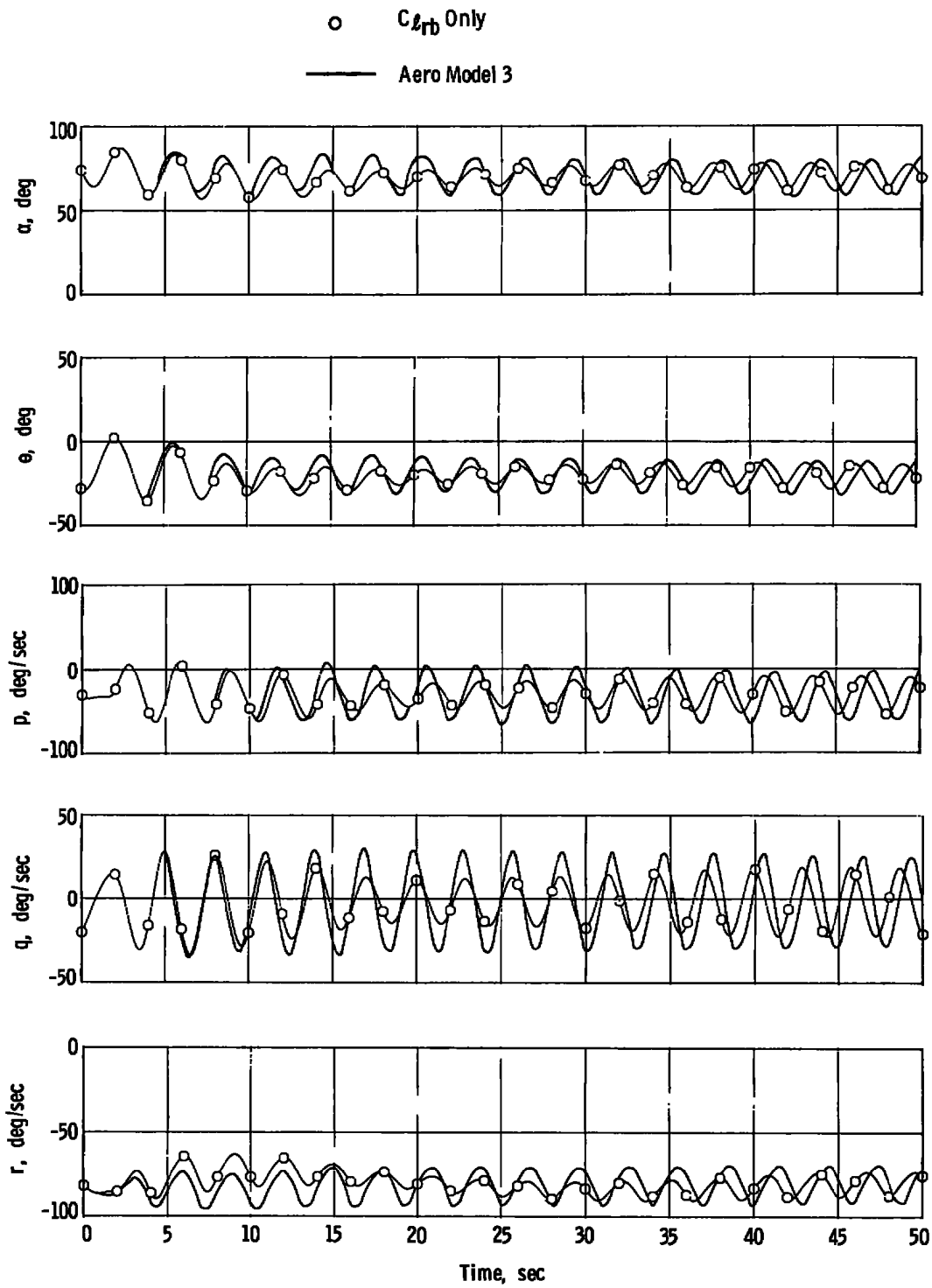

Figure 8. Comparison of calculated motions using Aero Model 3 system with $\Delta C_{\ell_{rb}}$ only and rotation-balance data.

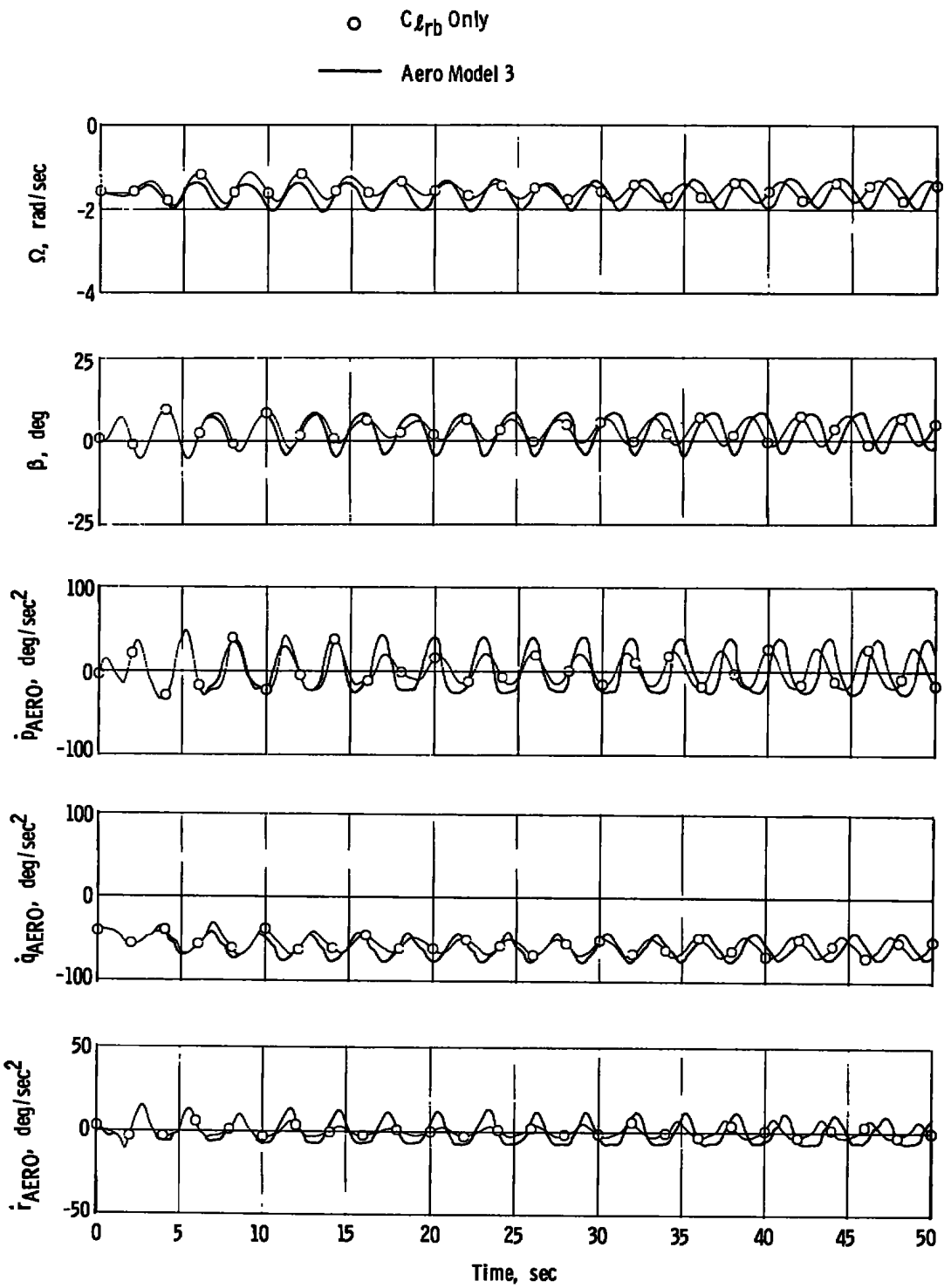

Figure 8. Concluded.

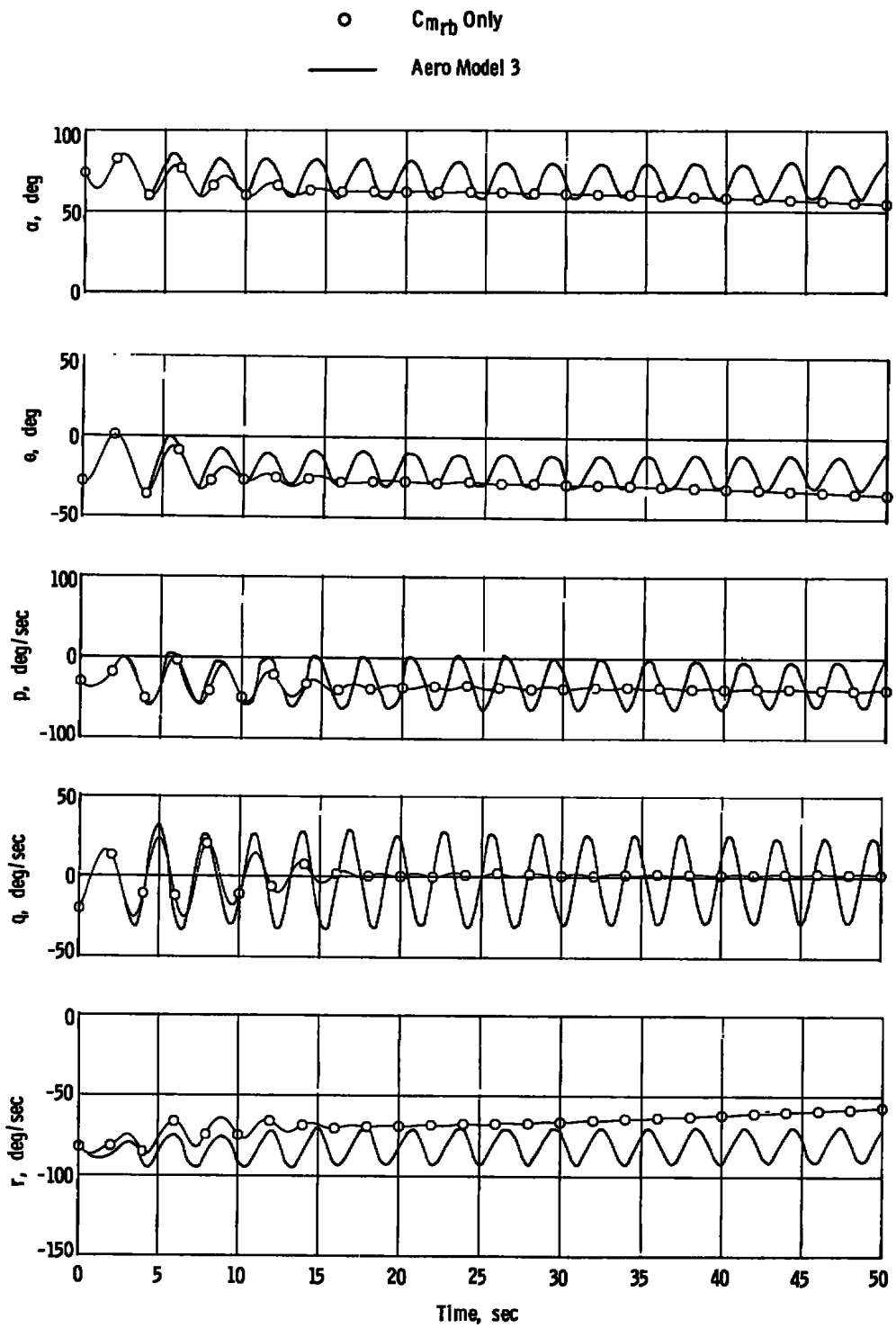

Figure 9. Comparison of calculated motions using Aero Model 3 system with $\Delta C_{m_{rb}}$ only and rotation-balance data.

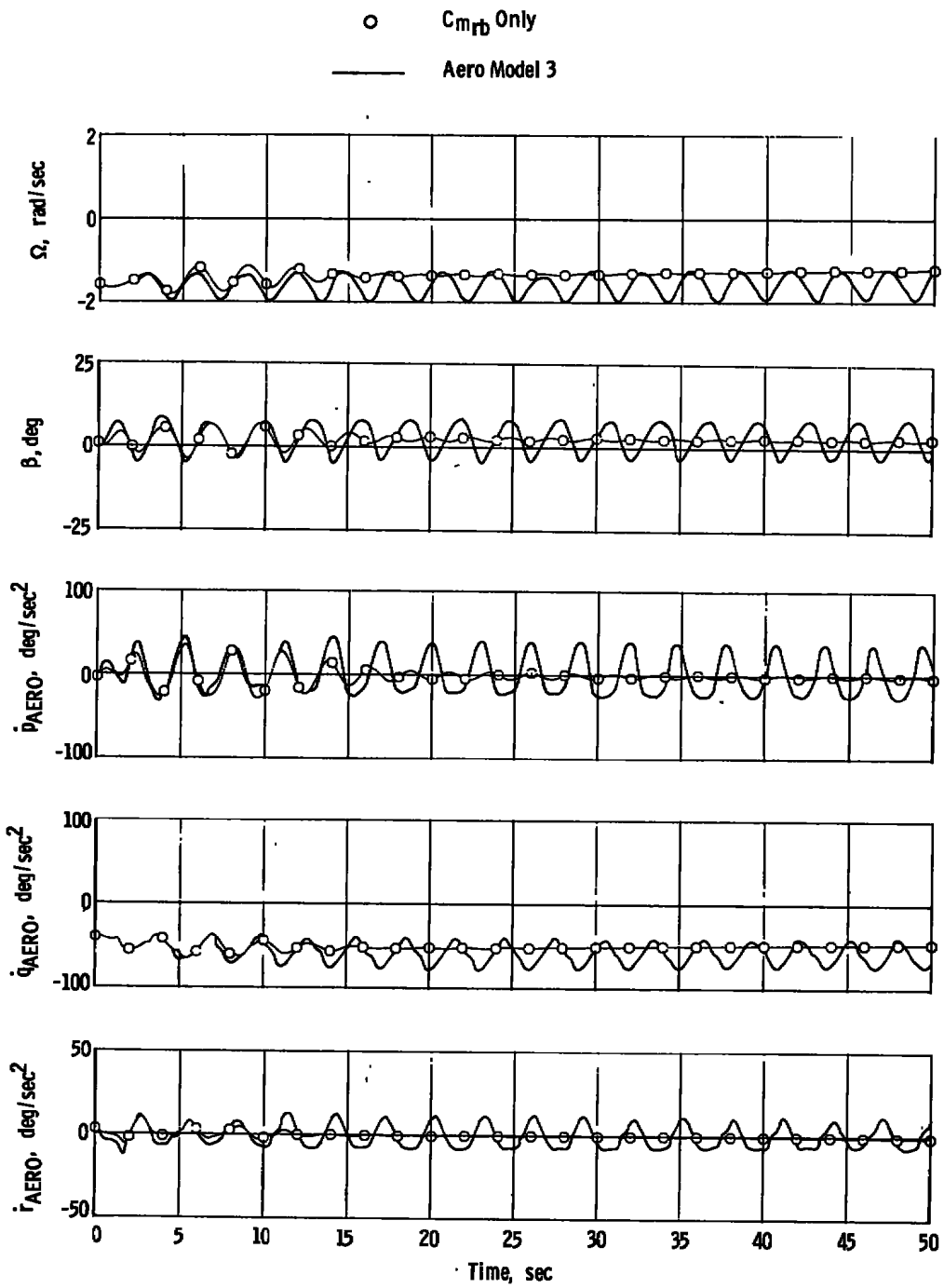

Figure 9. Concluded.

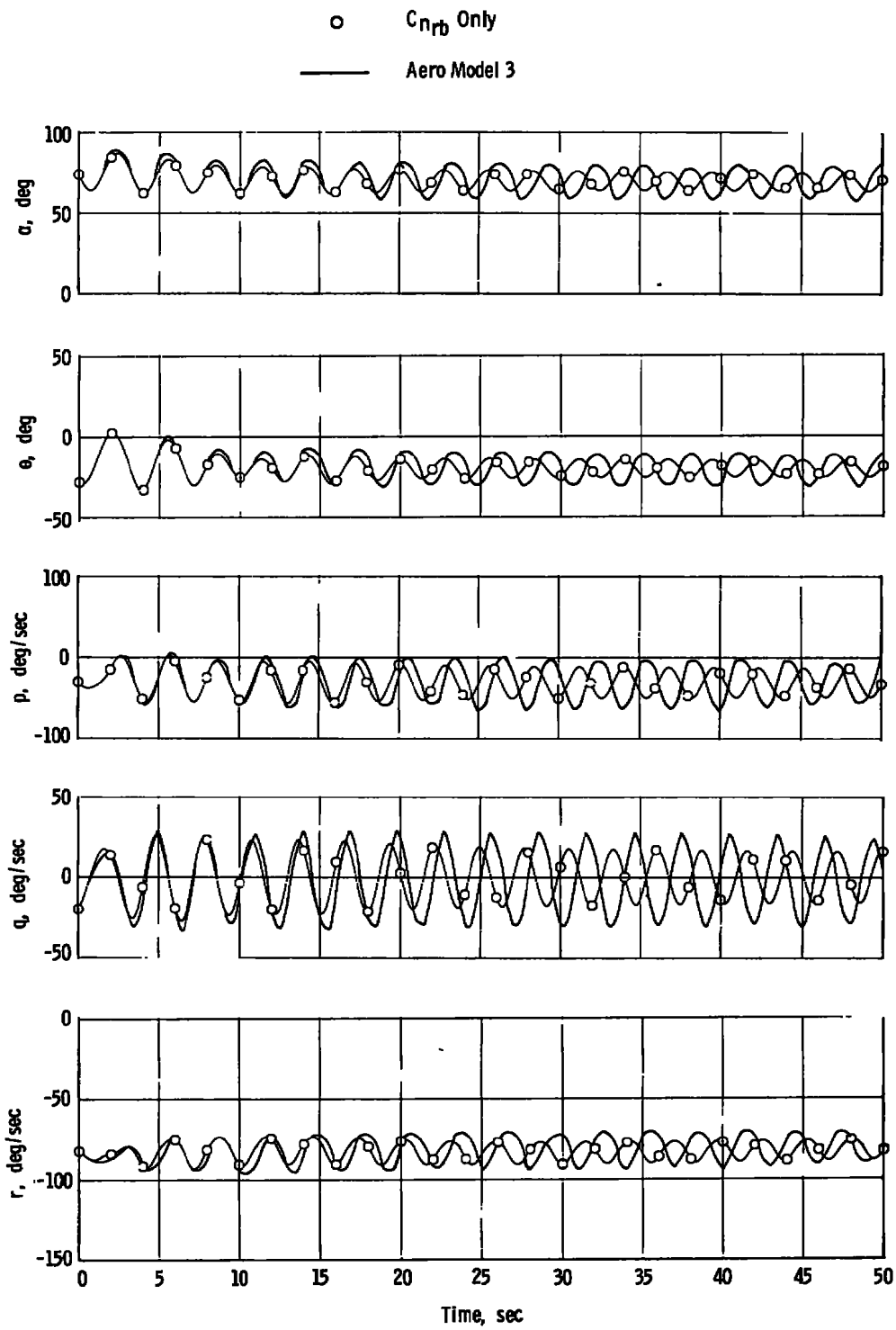

Figure 10. Comparison of calculated motion using Aero Model 3 system with $\Delta C_{n_{rb}}$ only and rotation-balance data.

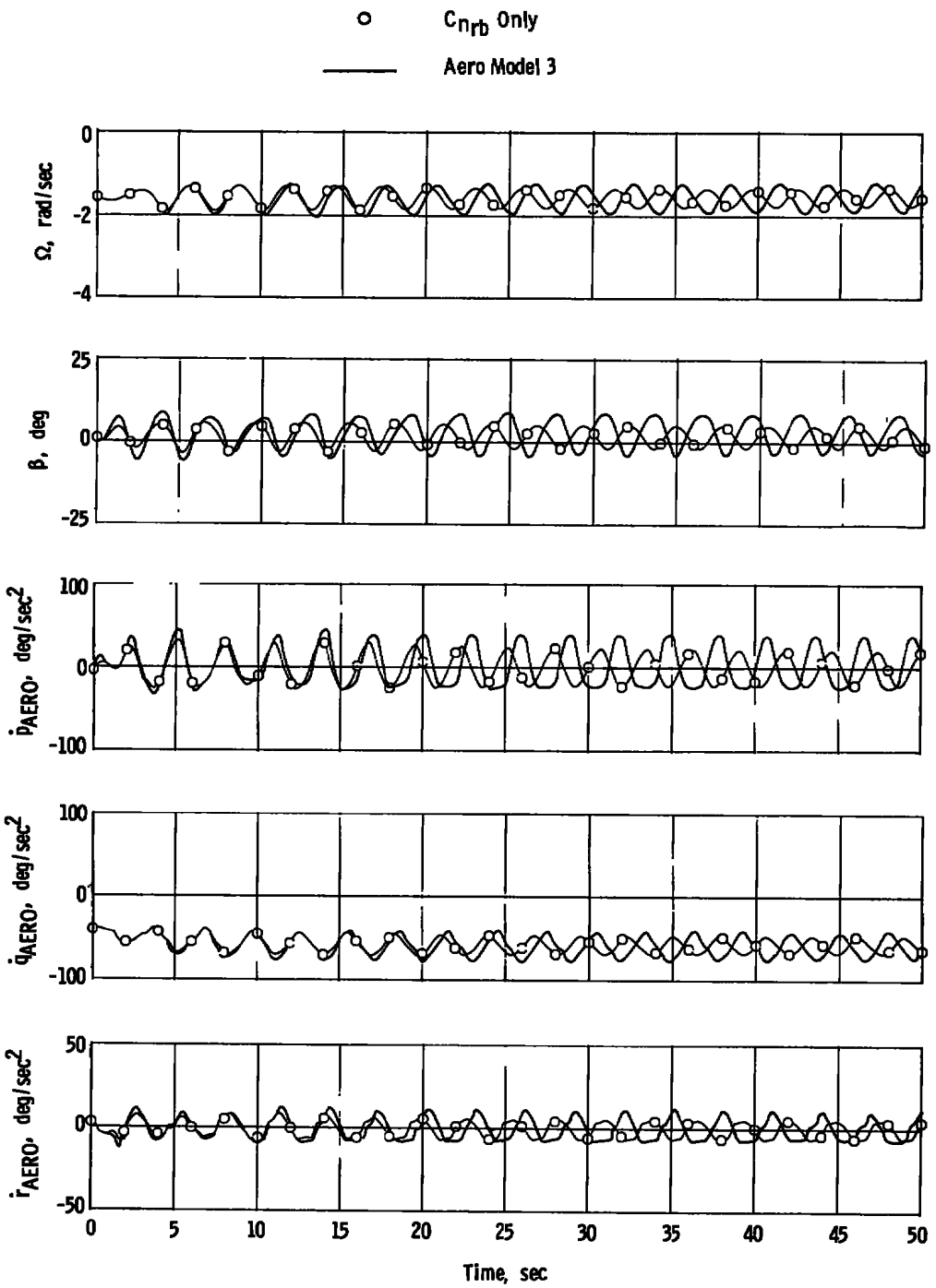

Figure 10. Concluded.

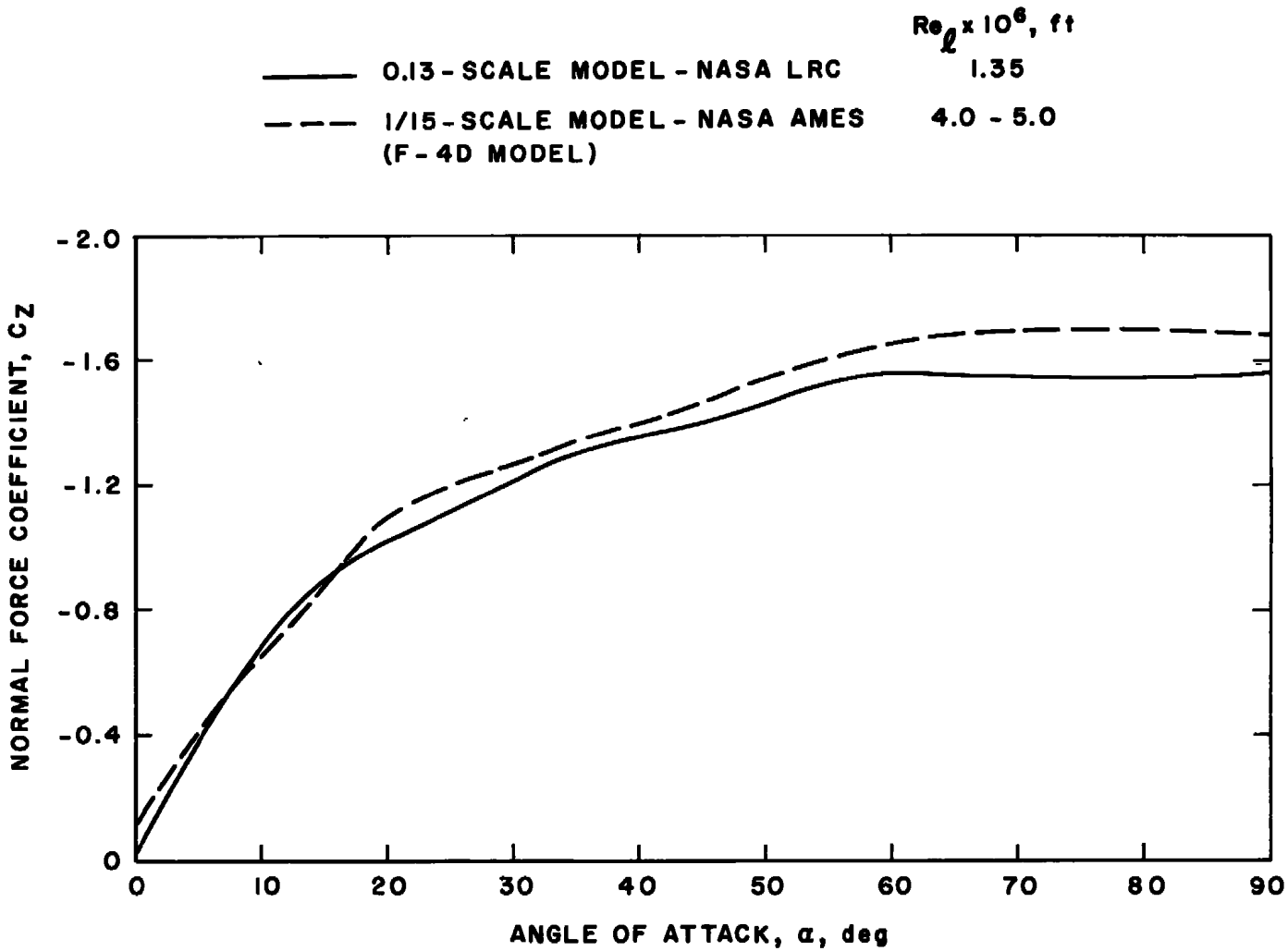

Figure 11. Comparison of NASA Ames and NASA Langley static normal-force coefficient, controls neutral position.

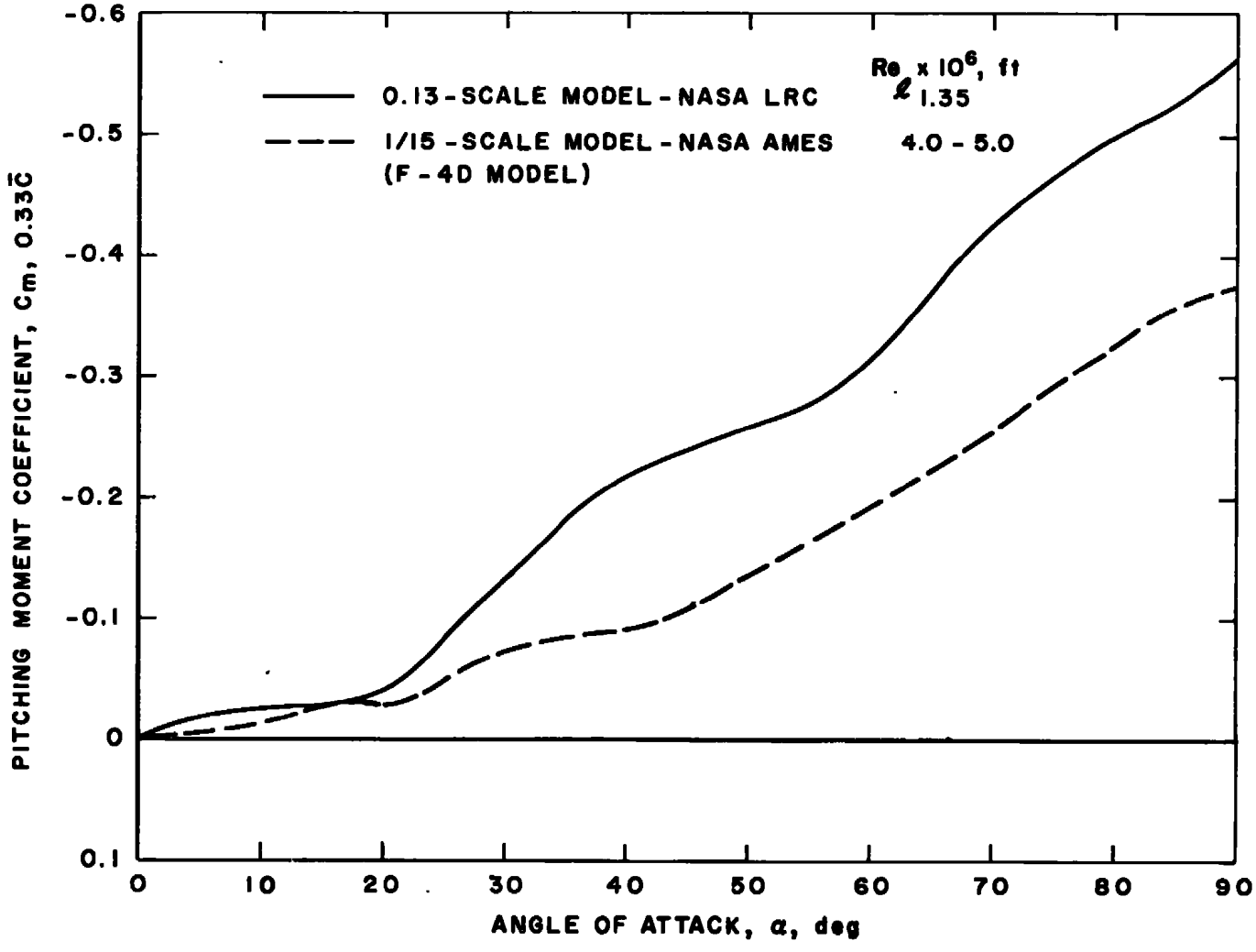

Figure 12. Comparison of NASA Ames and NASA Langley static pitching-moment coefficient, controls neutral position.

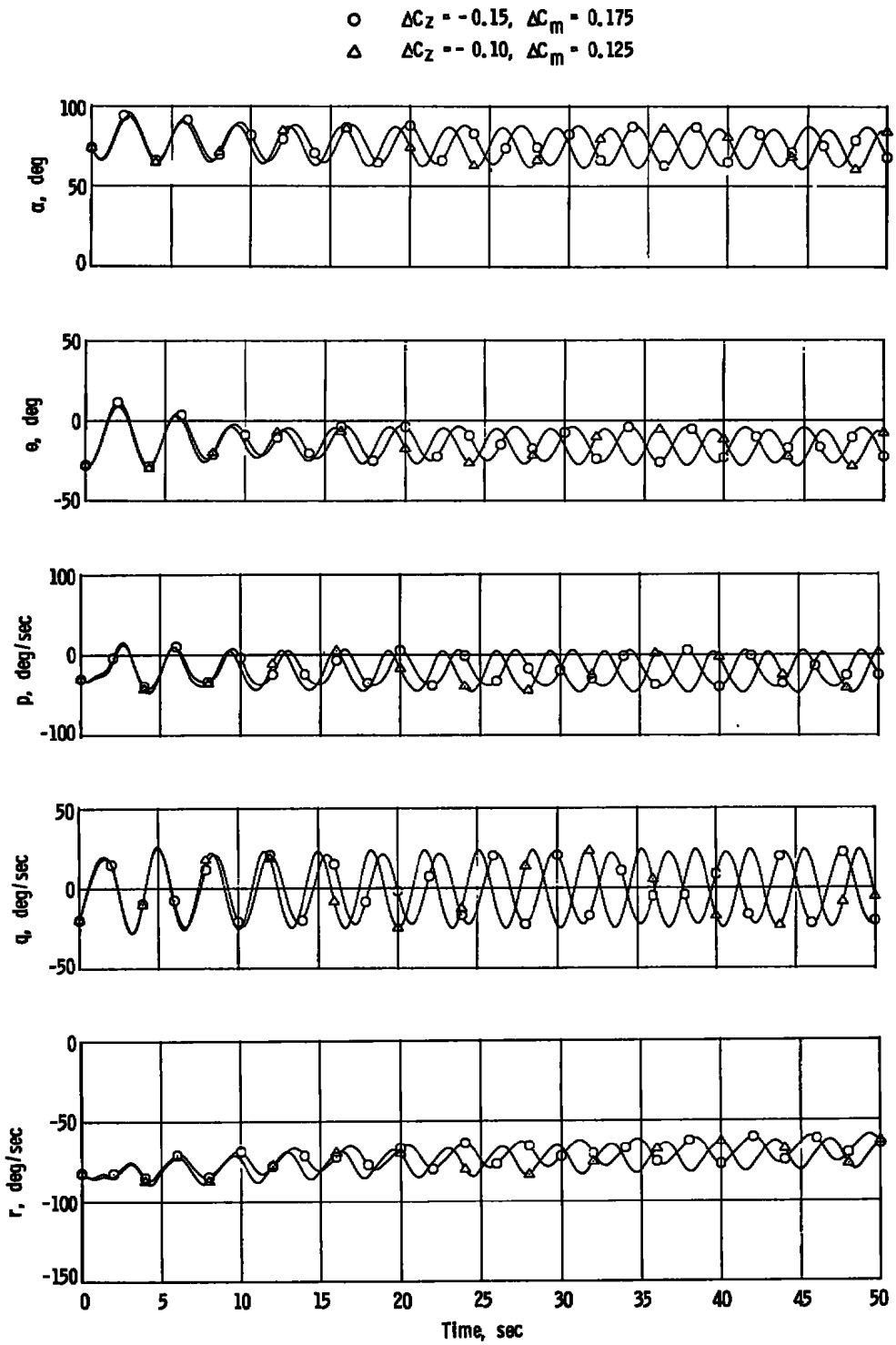

Figure 13. Comparison of calculated motions using Aero Model 3 for longitudinal coefficient increments.

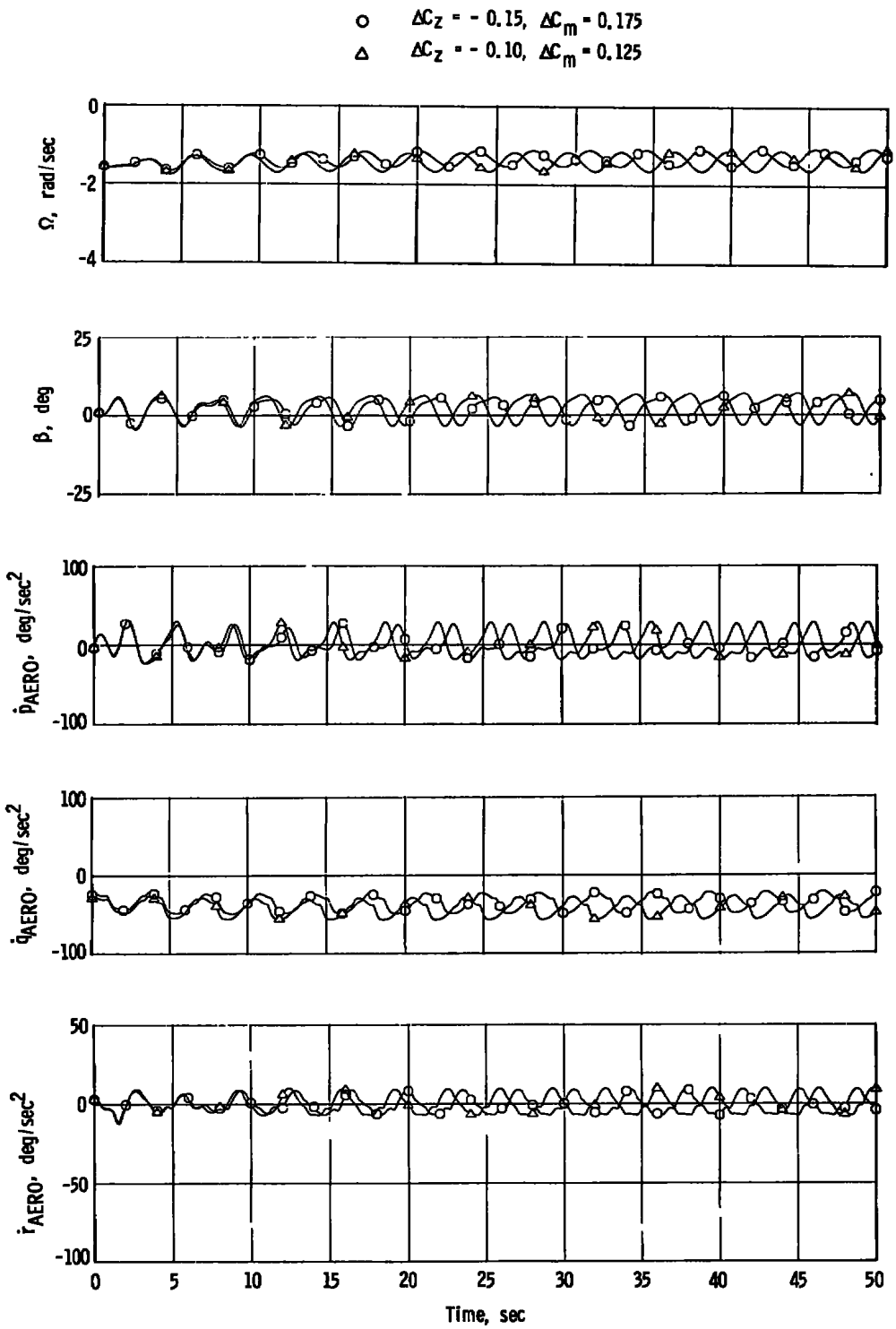

Figure 13. Concluded.

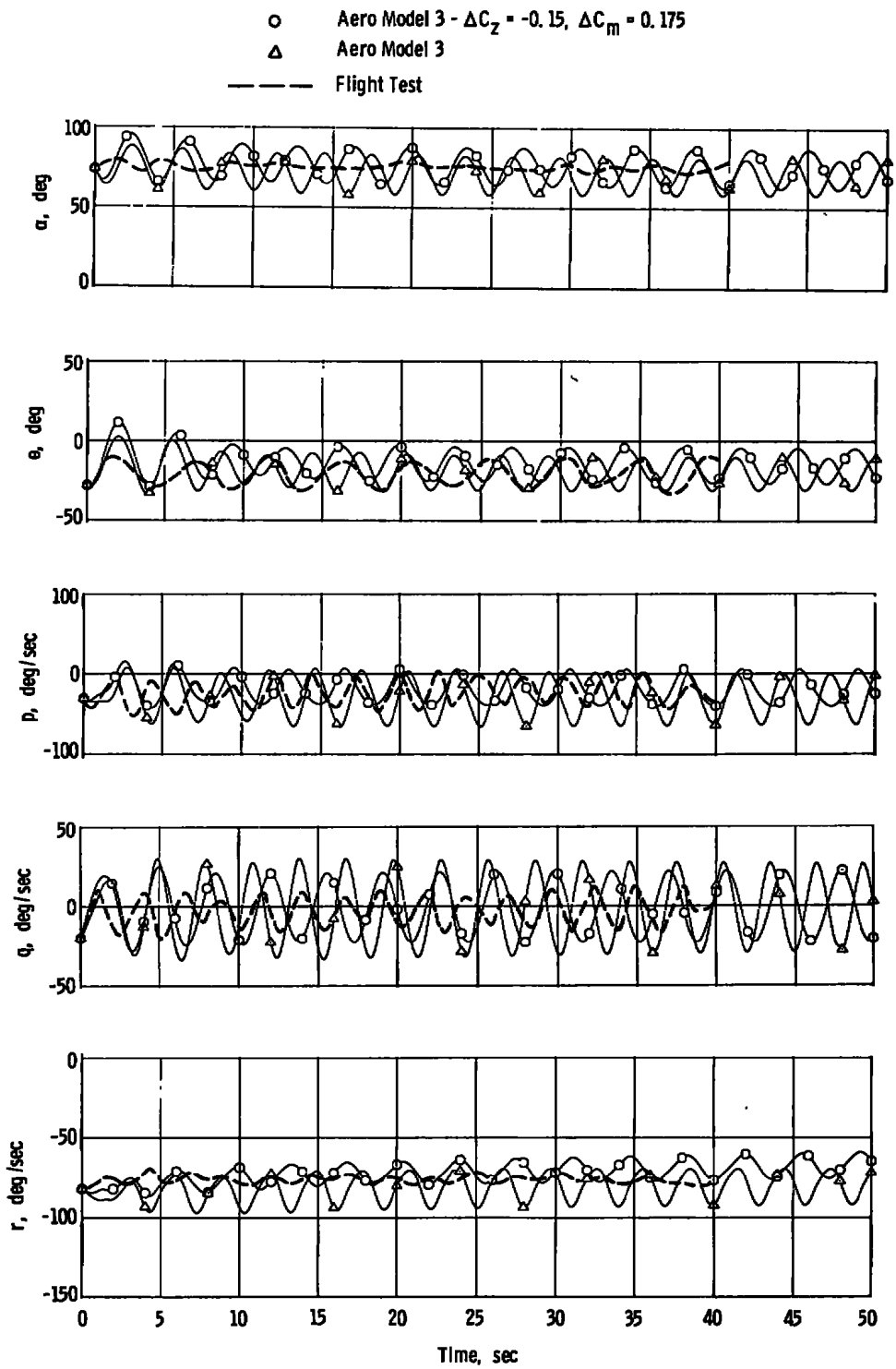

Figure 14. Comparison of calculated motions using Aero Model 3 with and without longitudinal increments and flight test.

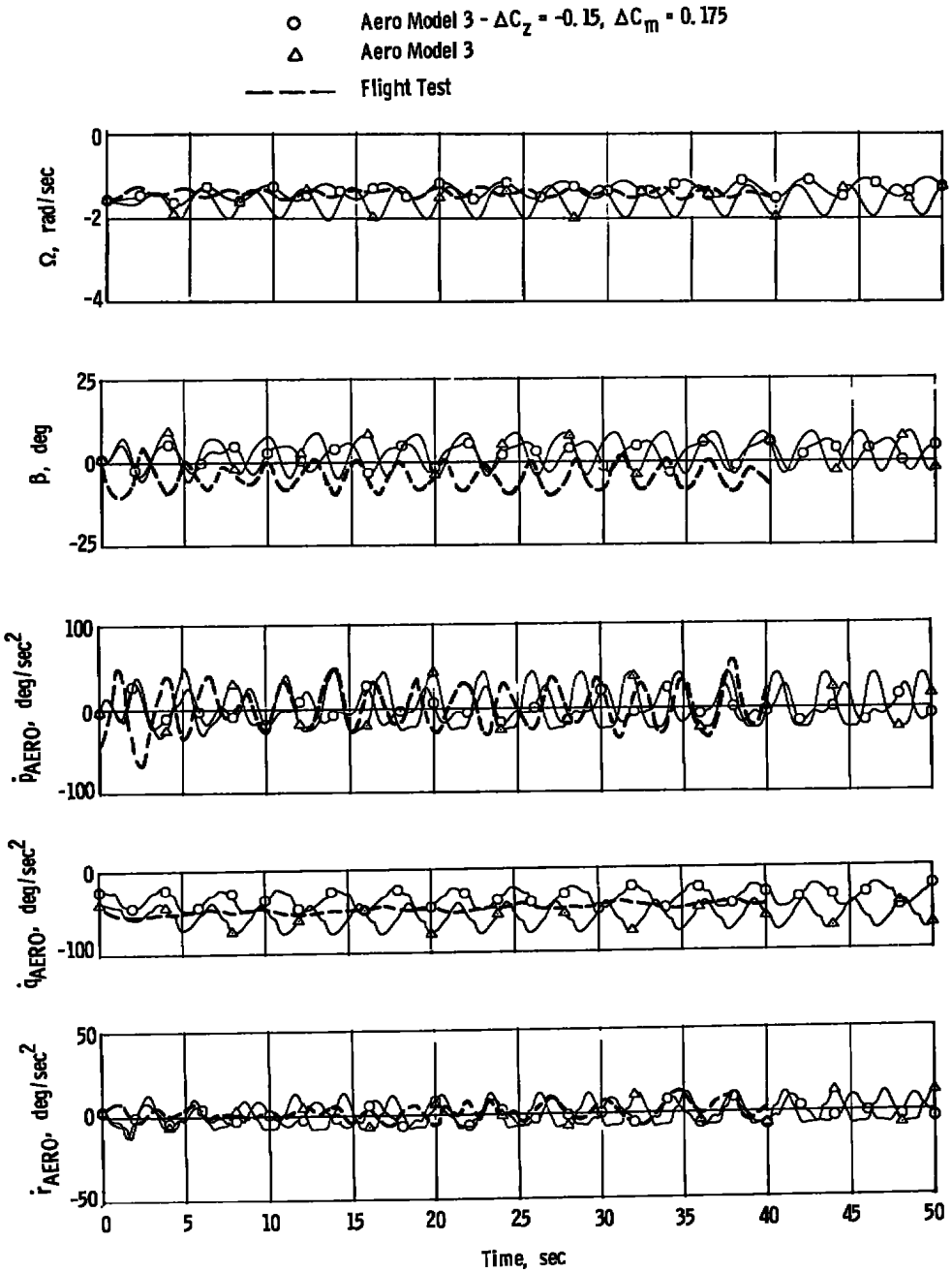

Figure 14. Concluded.

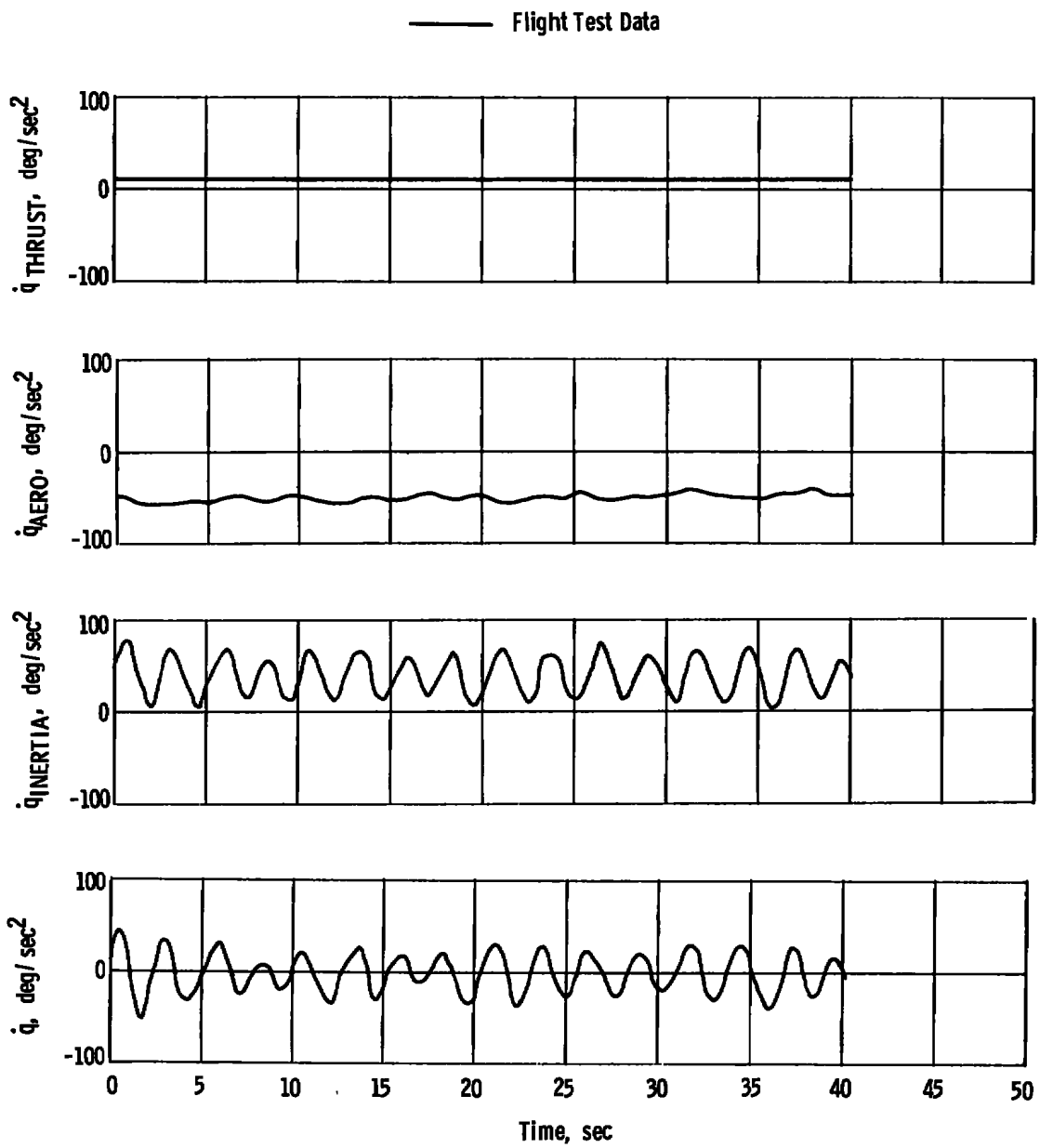

Figure 15. Components of flight test pitch angular acceleration.

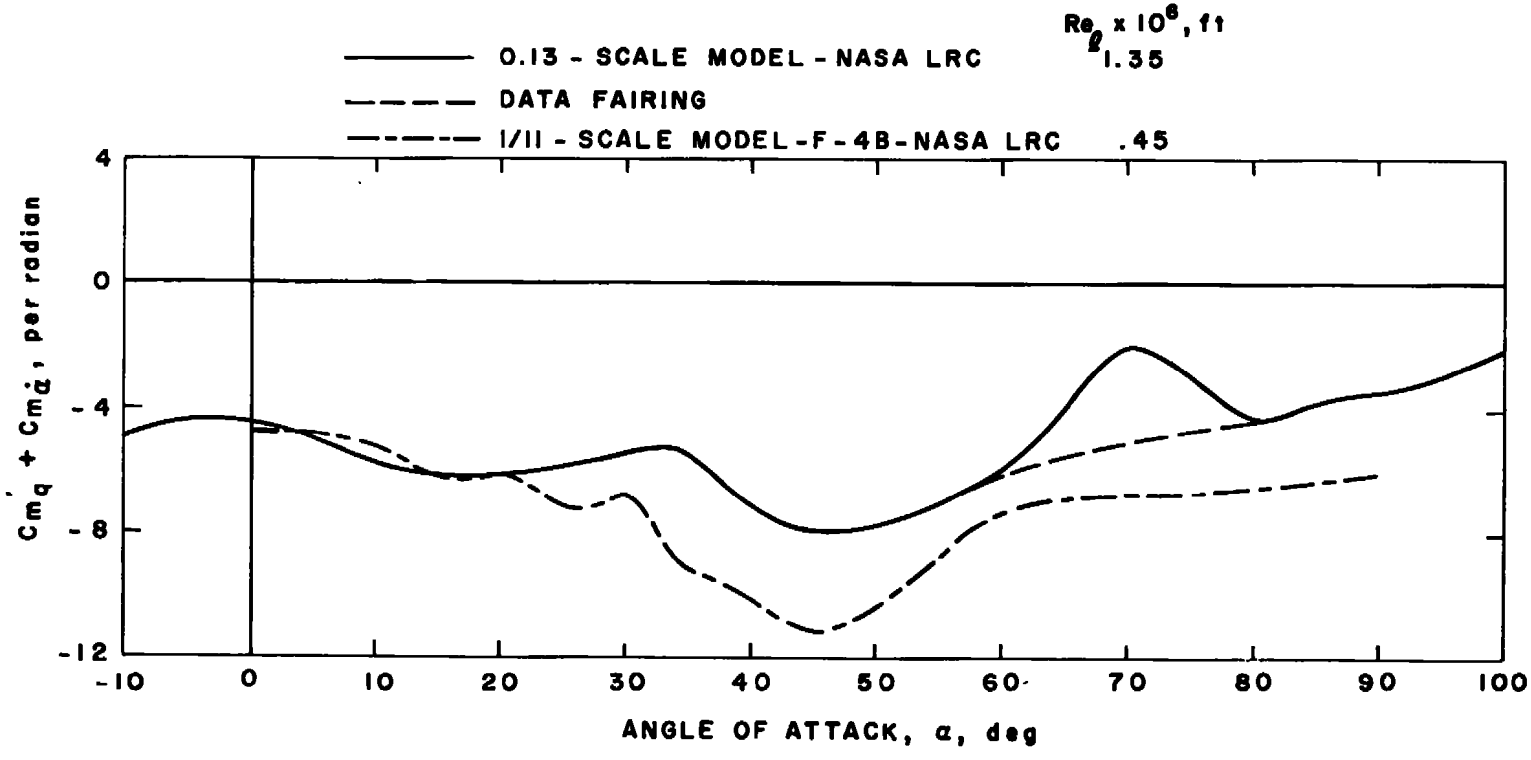

Figure 16. Variation of aerodynamic damping in pitch with angle of attack.

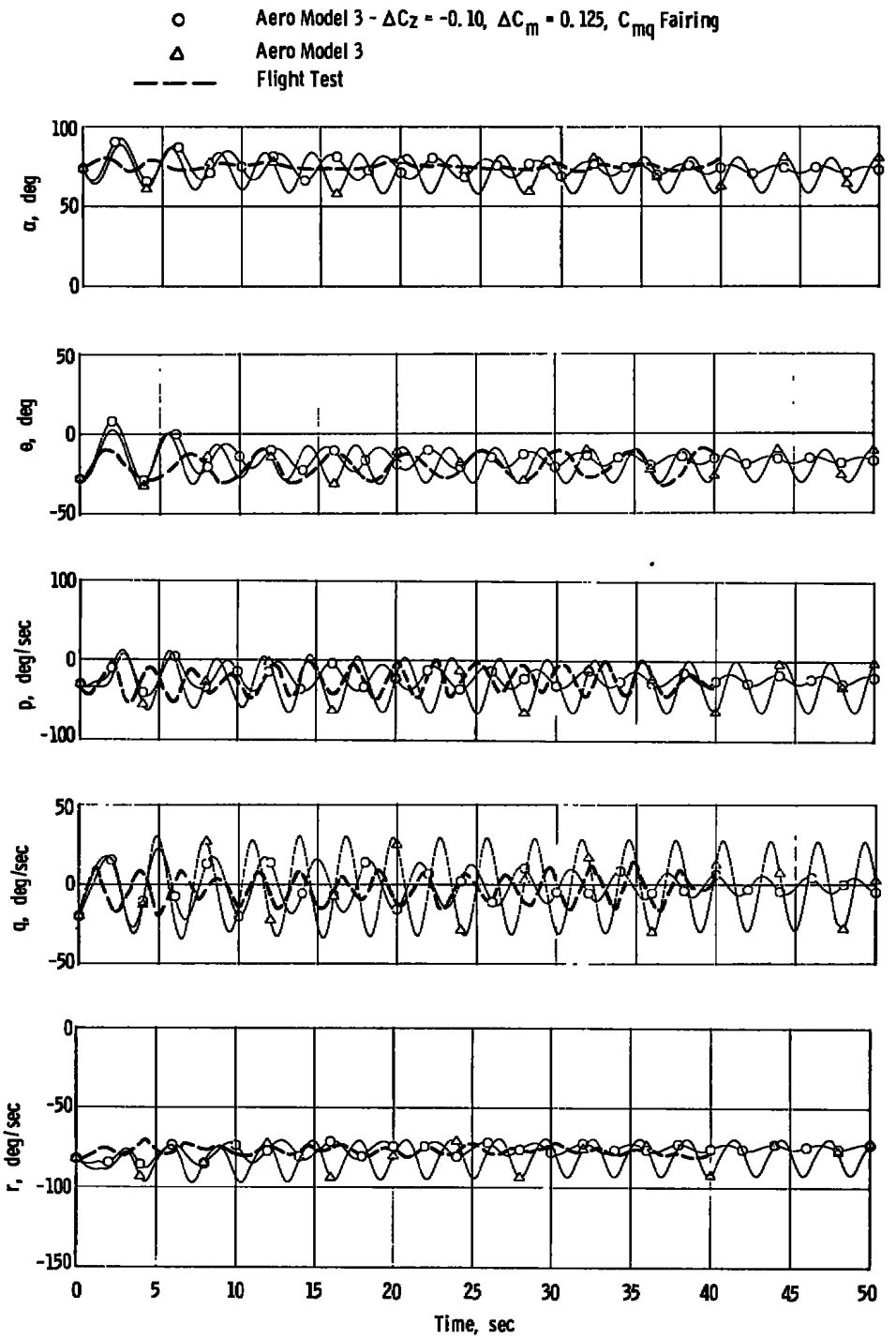

Figure 17. Comparison of calculated motions using Aero Model 3 with and without modifications in the static and pitch-damping data and flight test.

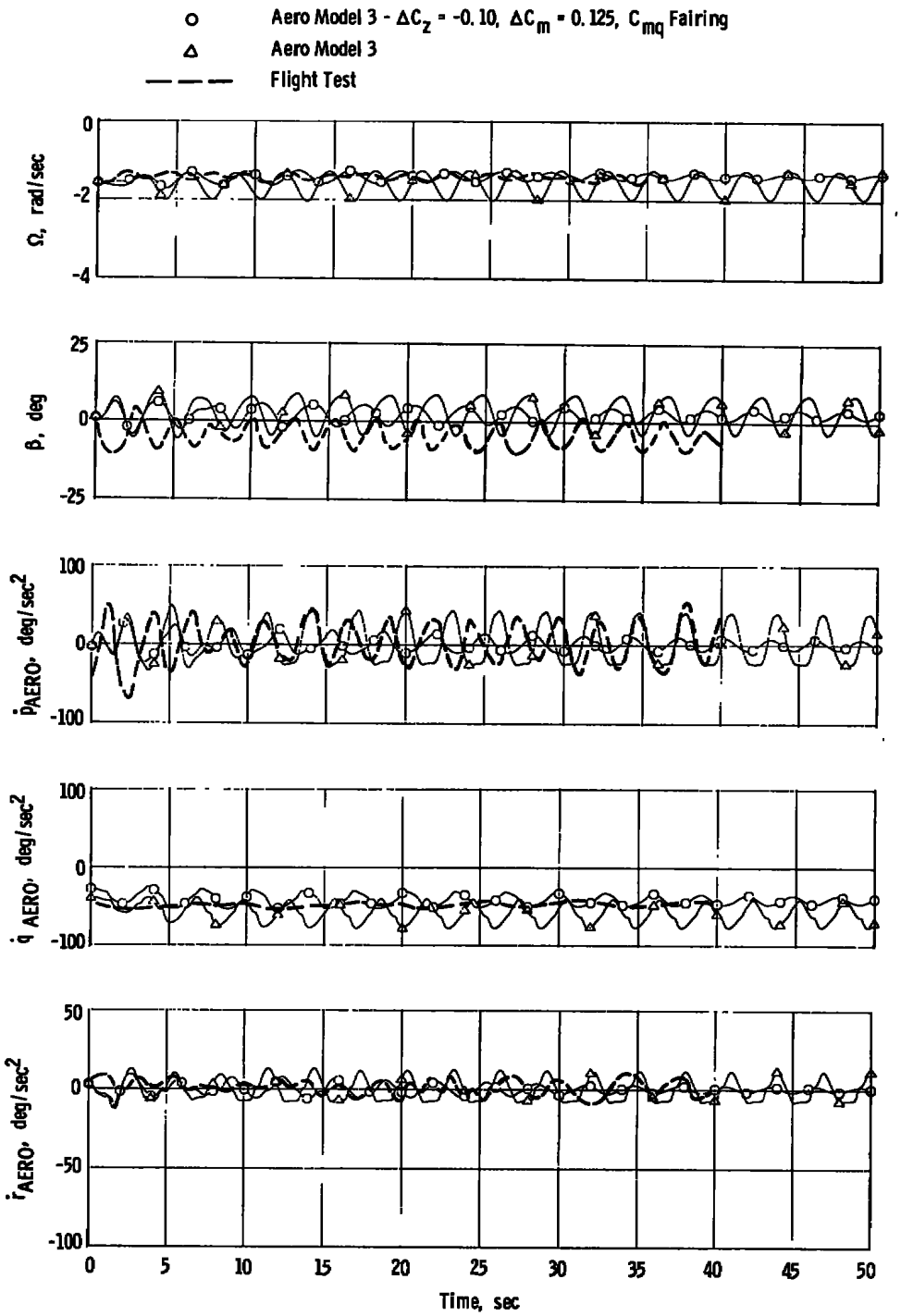

Figure 17. Concluded.

Table 1. Mass, Inertia, and Dimensional Characteristics of the F-4 aircraft

Loading – AIM-7's on Armament Stations 3 and 7	
Weight, lb	36,950
cg, percent MAC	33.7
Moments of Inertia, slug-ft^2	
I_X	22,600
I_Y	163,100
I_Z	182,000
I_{XZ}	5,450
Wing:	
Span, ft	38.41
Area, ft^2	538.34
Mean Aerodynamic Chord, ft	16.04

Inertia Coupling terms:

$$\frac{I_Y - I_Z}{I_X} = -0.836 \qquad \frac{I_{XZ}}{I_X} = 0.241$$

$$\frac{I_Z - I_X}{I_Y} = 0.977 \qquad \frac{I_{XZ}}{I_Y} = 0.033$$

$$\frac{I_X - I_Y}{I_Z} = -0.772 \qquad \frac{I_{XZ}}{I_Z} = 0.030$$

Table 2. Initial Conditions from Flight 202, Run 12 of Ref. 12

Conditions at 85 sec in the Spin:

α = 74 deg	$\dot{p}$ = −62.0 deg/sec^2
β = 1 deg	$\dot{r}$ = −11.0 deg/sec^2
θ = −28.0 deg	h = 12,500 ft
ϕ = 8.0 deg	$\bar{q}$ = 35 lb/ft^2
ψ = 0 deg	M_∞ = 0.18
q = −20.0 deg/sec	d = −0.3866 ft
p = −30.0 deg/sec	T = 62 lb (at Idle rpm)
r = −82.0 deg/sec	I_{XE} = 42 slug-ft^2
$\dot{q}$ = 15.0 deg/sec^2	Φ_E = 518.0 rad/sec

ϵ = 5.25 deg

Controls Time Function:

Time, sec	0.0 →	50.0
δ_H, deg	3.0 →	3.0
δ_r, deg	0.0 →	0.0
δ_α, deg	0.0 →	0.0

APPENDIX A
EQUATIONS OF MOTION

A.1 SIX-DEGREE-OF-FREEDOM, RIGID-BODY EQUATION OF MOTIONS

The dynamic equations required to specify the translational and rotational motions of a rigid body moving through space are described in this appendix. The six-degree-of-freedom nonlinear differential equations representing linear and angular accelerations on a moving body axis system (Fig. A-1) having its origin at the aircraft center of mass are presented below.

Forces:

$$\dot{u} = rv - qw - g \sin\theta + \frac{F_x}{m} - \frac{T_x}{m}$$

$$\dot{v} = pw - ru + g \cos\theta \sin\phi + \frac{F_Y}{m}$$

$$\dot{w} = qu - pv + g \cos\theta \cos\phi + \frac{F_z}{m} + \frac{T_z}{m}$$

Moments:

$$\dot{p} = \frac{I_Y - I_Z}{I_X} qr + \frac{I_{XZ}}{I_X} (\dot{r} + pq) + \frac{M_X}{I_X}$$

$$\dot{q} = \frac{I_Z - I_X}{I_Y} pr + \frac{I_{XZ}}{I_Y} (r^2 - p^2) + \frac{M_Y}{I_Y} + \frac{M_{YT}}{I_Y} + \frac{M_{YG}}{I_Y}$$

$$\dot{r} = \frac{I_X - I_Y}{I_Z} pq + \frac{I_{XZ}}{I_Z} (\dot{p} - qr) + \frac{M_Z}{I_Z} + \frac{M_{ZG}}{I_Z}$$

The external forces and moments (F_X, F_Y, F_Z, M_X, M_Y, and M_Z) in the equations are comprised of aerodynamic coefficients representative of the aircraft. The external force and moment contributions due to engine thrust (including gyroscopic effect) are represented by T_X, T_Z, M_{YT}, M_{YG}, and M_{ZG} and are developed in Appendix A.2. Development of the aerodynamic math model used is presented in Appendix A.3. The method used in implementing the rotational-balance data is outlined in Appendix B.

Auxiliary equations used in this analysis are given as follows:

$$\alpha = \tan^{-1}\left(\frac{w}{u}\right), \qquad \beta = \sin^{-1}\left(\frac{v}{V}\right)$$

$$\dot{\alpha} = \frac{u\dot{w} - w\dot{u}}{u^2 + w^2}, \qquad \dot{\beta} = \dot{v} - \frac{v}{V^2}\left(\frac{u\dot{u} + v\dot{v} + w\dot{w}}{\sqrt{u^2 + w^2}}\right)$$

$$V = \sqrt{u^2 + v^2 + w^2}, \qquad \gamma = \tan^{-1}\left(\frac{\dot{h}}{\sqrt{\dot{x}^2 + \dot{y}^2}}\right)$$

$$\dot{\theta} = q\cos\phi - r\sin\phi$$

$$\dot{\phi} = p - \tan\theta\,(r\cos\phi + q\sin\phi)$$

$$\dot{\psi} = \frac{r\cos\phi + q\sin\phi}{\cos\theta}$$

$$\Omega_{ss} = \frac{up + vq + wr}{|V|}$$

An explanation of the steady-state rotational rate vector ($\vec{\Omega}_{ss}$) is given in Appendix B.2.

The equations of motion are numerically intergrated to provide time histories of the aircraft spinning motion.

A.2 EQUATIONS DEFINING THE FORCE AND MOMENT CONTRIBUTIONS DUE TO ENGINE THRUST

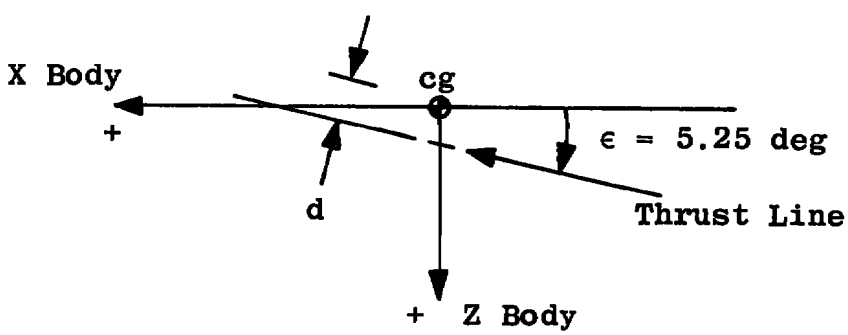

Forces	Moments
$T_X = T \cos \epsilon$	$M_{XT} = 0$
$T_Y = 0$	$M_{YT} = T(d)$
$T_Z = -T \sin \epsilon$	$M_{YG} = -I_{XE}\phi_E r$
	$M_{ZG} = I_{XE}\phi_E q$

where

ϕ_E = Engine rotor angular velocity, rad/sec

I_{XE} = Engine rotor moment of inertia, slug/ft^2

d = Distance between thrust line and cg

Assumptions

1. Engine thrust line parallel to X-Z plane.
2. Gyroscopic moments assume engine axis parallel to X axis.
3. No variation in Y and Z cg location.

A.3 EQUATIONS DEFINING THE TOTAL AERODYNAMIC DATA ALONG AND ABOUT EACH BODY AXIS

LONGITUDINAL AXIS PLANE

$$F_X = \bar{q}S\left[C_x(\alpha, \beta, \delta_H) + \Delta C_{x_{rb}}\left(\alpha, \beta, \delta_H, \frac{\Omega_{ss}b}{2V}\right) + \left(C_{x_q}(\alpha)\right)\frac{q_o C}{2V}\right]$$

$$F_Z = \bar{q}S\left[C_z(\alpha, \beta, \delta_H) + \Delta C_{z_{rb}}\left(\alpha, \beta, \delta_H, \frac{\Omega_{ss}b}{2V}\right) + \left(C_{z_q}(\alpha)\right)\frac{q_o C}{2V}\right]$$

$$M_Y = \bar{q}SC\left[C_m(\alpha, \beta, \delta_H) + \Delta C_{m_{rb}}\left(\alpha, \beta, \delta_H, \frac{\Omega_{ss}b}{2V}\right) + \left(C_{m_q}(\alpha)\right)\frac{q_o C}{2V}\right.$$

$$\left. + C_{m_p}\left(\frac{p_o b}{2V}\right) + C_{m_r}\left(\frac{r_o b}{2V}\right)\right]$$

LATERAL-DIRECTIONAL AXIS PLANE

$$F_Y = \bar{q}S\left[C_y(\alpha, \beta) + \Delta C_y(\alpha, \beta, \delta_r) + \Delta C_{y_{rb}}\left(\alpha, \beta, \frac{\Omega_{ss}b}{2V}\right)\right.$$

$$\left. + \left(C_{y_p}(\alpha)\right)\frac{p_o b}{2V} + \left(C_{y_r}(\alpha, \delta_H)\right)\frac{r_o b}{2V}\right]$$

$$M_Z = \bar{q}Sb\left\{C_n(\alpha, \beta) + \Delta C_n(\alpha, \beta, \delta_a) + \Delta C_n(\alpha, \beta, \delta_r)\right.$$

$$+ \Delta C_{n_{rb}}\left(\alpha, \beta, \frac{\Omega_{ss}b}{2V}\right) + \left[C_{n_p}(\alpha)\right]\frac{p_o b}{2V} + \left[C_{n_r}(\alpha, \delta_H)\right]\frac{r_o b}{2V}$$

$$\left. + C_{n_{\dot{\beta}}}\frac{\dot{\beta}b}{2V} + C_{n_q}\frac{q_o C}{2V}\right\}$$

$$M_X = \bar{q}Sb\left\{C_\ell(\alpha, \beta) + \Delta C_\ell(\alpha, \beta, \delta_a) + \Delta C_\ell(\alpha, \beta, \delta_r)\right.$$

$$+ \Delta C_{\ell_{rb}}\left(\alpha, \beta, \frac{\Omega_{ss}b}{2V}\right) + \left[C_{\ell_p}(\alpha)\right]\frac{p_o b}{2V} + \left[C_{\ell_r}(\alpha, \delta_H)\right]\frac{r_o b}{2V}$$

$$\left. + C_{\ell_{\dot{\beta}}}\frac{\dot{\beta}b}{2V} + C_{\ell_q}\frac{q_o C}{2V}\right\}$$

where

$\Delta C_\ell(\alpha, \beta, \delta_a) = \Delta C_\ell(\alpha, \beta, 30)\left(\frac{\delta_a}{30}\right)$, surface command determines whether left or right roll command.

$\Delta C_\ell(\alpha, \beta, \delta_r) = \Delta C_\ell(\alpha, \beta, \pm 30)\left(\frac{\delta_r}{30}\right)$

where the "Δ" equations are the same as for C_ℓ above except C_ℓ is replaced by C_y or C_n.

A.4 EQUATIONS FOR TRANSFERRING AERODYNAMIC DATA INPUTS TO THE PROPER HORIZONTAL CENTER OF GRAVITY POSITION

$$M_{X_{cg}} = M_X$$

$$M_{Y_{cg}} = M_Y - F_Z \text{ (RDELCG)}$$

$$M_{Z_{cg}} = M_Z + F_Y \text{ (RDELCG)}$$

where

$$\text{RDELCG} = (cg_{NEW} - cg_{REF})\ C, \text{ ft}$$

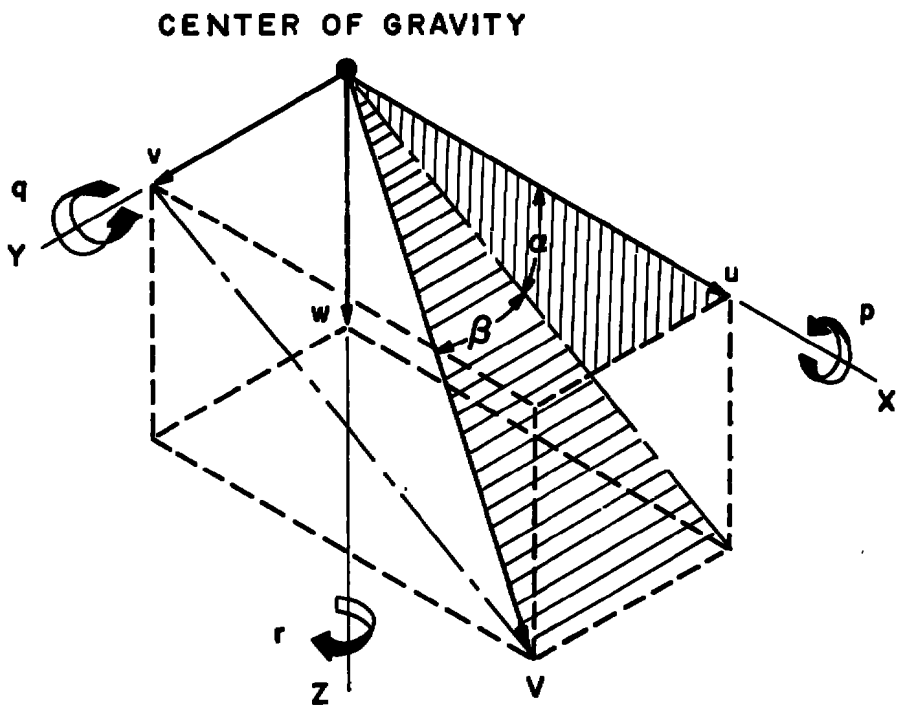

Figure A-1. Body axis system.

APPENDIX B
IMPLEMENTATION METHODS FOR ROTATION-BALANCE DATA

B.1 ADDITION OF INCREMENTAL ROTATION-BALANCE DATA TO AERODYNAMIC FORCE AND MOMENT EQUATION

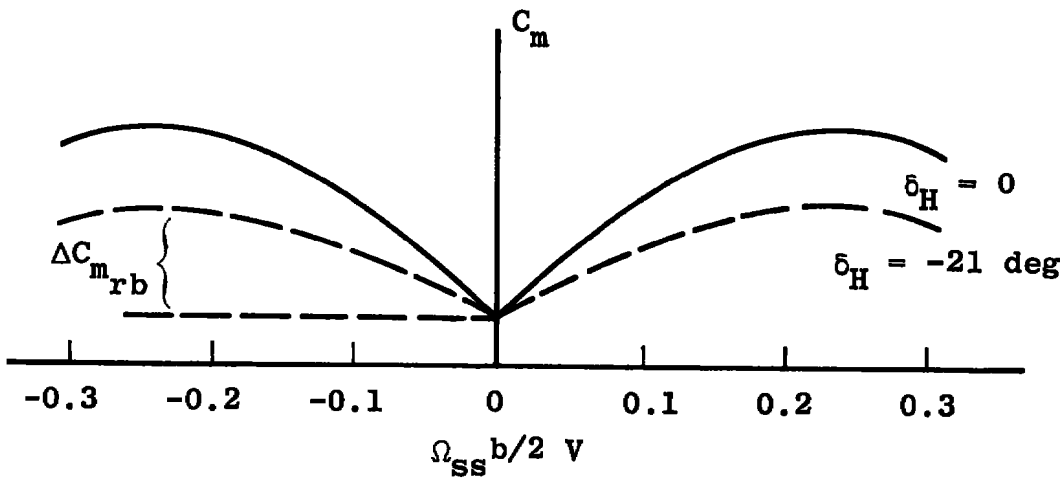

$$\Delta C_{m_{rb}}\left(\alpha, \beta, \delta_H, \frac{\Omega_{ss}b}{2V}\right) = \Delta C_{m_{rb}}\left(\alpha, \beta, 0, \frac{\Omega_{ss}b}{2V}\right) + \left|\frac{\delta_H}{-21}\right| \left[\Delta C_{m_{rb}}\left(\alpha, \beta, -21, \frac{\Omega_{ss}b}{2Y}\right) - \Delta C_{m_{rb}}\left(\alpha, \beta, 0, \frac{\Omega_{ss}b}{2V}\right)\right]$$

where

$\Delta C_{m_{rb}}\left(\alpha, \beta, 0, \frac{\Omega_{ss}b}{2Y}\right)$ = incremental rotation–balance data for longitudinal control surface neutral

$\Delta C_{m_{rb}}\left(\alpha, \beta, -21, \frac{\Omega_{ss}b}{2V}\right)$ = incremental rotation–balance data for longitudinal control surface at -21 deg

For other coefficients, replace C_m with C_X, C_Z, C_Y, C_n, or C_ℓ.

B.2 EQUATIONS DEFINING THE STEADY-STATE ROTATIONAL RATE VECTOR

The rotation-balance data incorporated in the aerodynamic data model of Appendix A.3 were obtained with a model/balance rotating in the wing tunnel with its rotational vector aligned with the velocity vector of the wind tunnel. Because the rotational and velocity vectors are normally not aligned in spinning flight, the direct implementation of the rotation balance data as a function of the total rotational rate vector ($\vec{\Omega}$) is in error. The method used for implementing the data resolves a component of the total rotational vector along the aircraft velocity vector. This component rotational vector ($\vec{\Omega}_{ss}$) may now be used in determining the incremental coefficients to be included in the aerodynamic data matrices. The determination of the magnitude of the steady-state rotational vector ($\vec{\Omega}_{ss}$) and its inclination (δ) to the aircraft total rotational vector ($\vec{\Omega}$) is outlined below and is the same as that used in Ref. 15.

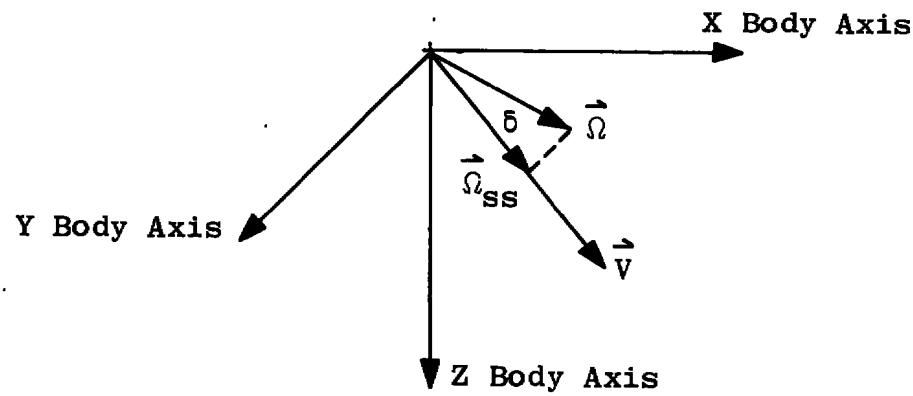

$\vec{v} = u\vec{i} + v\vec{j} + w\vec{k}$ = Total velocity vector

$\vec{\Omega} = p\vec{i} + q\vec{j} + r\vec{k}$ = Total rotational vector

$\vec{\Omega}_{ss} = p_{ss}\vec{i} + q_{ss}\vec{j} + r_{ss}\vec{k}$ = Steady-state rotational vector along velocity vector $\vec{V}$.

$$|\Omega_{ss}| = |\Omega| \cos\delta, \quad \cos\delta = \frac{|\Omega_{ss}|}{|\Omega|}$$

$$\vec{\Omega} \cdot \vec{V} = |\Omega|\,|V| \cos\delta$$

$$up - vq + wr = |\Omega|\,|V| \cos\delta$$

Now substituting,

$$|\Omega_{ss}| = \frac{up + vq + wr}{|V|}$$

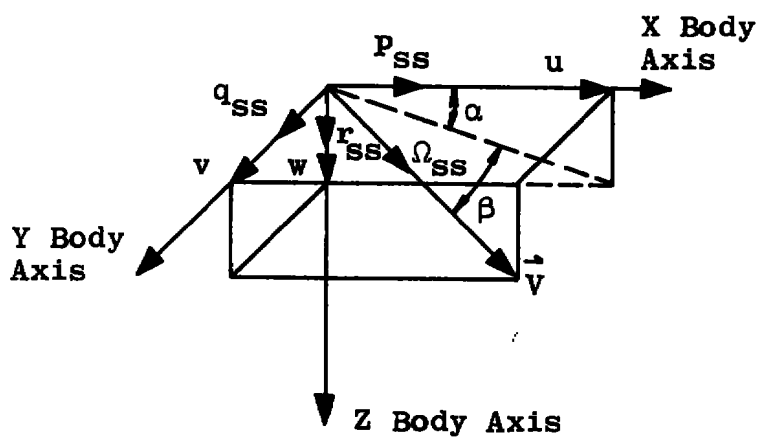

But

$$\frac{u}{v} = \cos\beta \cos\alpha$$

$$\frac{v}{V} = \sin\beta$$

$$\frac{w}{V} = \cos\beta \sin\alpha$$

again substituting,

$$\Omega_{ss} = p \cos\beta \cos\alpha + q \sin\beta + r \cos\beta \sin\alpha$$

To separate p, q, and r into steady-state (parallel to $\vec{V}$) and oscillatory (perpendicular to $\vec{V}$) components, the components of $\vec{\Omega}_{ss}$ along the X, Y, and Z axes are first determined.

$$\vec{\Omega}_{ss} = \vec{\Omega}_{ss} \frac{\vec{V}}{V}$$

$$\vec{\Omega}_{ss} = \Omega_{ss} \cos\beta \cos\alpha\, \vec{i} + \Omega_{ss} \sin\beta \vec{j} - \Omega_{ss} \cos\beta \sin\alpha\, \vec{k}$$

Components of Ω_{ss} in the $\vec{i}$, $\vec{j}$, and $\vec{k}$ directions are the steady-state components of p, q, and r, respectively.

Therefore

$$p_{ss} = \Omega_{ss} \cos\beta \cos\alpha$$

$$q_{ss} = \Omega_{ss} \sin\beta$$

$$r_{ss} = \Omega_{ss} \cos\beta \sin\alpha$$

The oscillatory components are:

$$p_o = p - p_{ss}$$

$$q_o = q - q_{ss}$$

$$r_o = r - r_{ss}$$

The oscillatory components are used in conjunction with the dynamic oscillatory derivatives in the aerodynamic data matrices of Appendix A.3. Utilizing the rotational and oscillatory derivatives in the manner outlined accounts for oscillations that are superimposed on an aircraft steady-state spinning motion.

In the subject investigation, the rotation-balance data were applied when the inclination angle (δ) between the rotational vector ($\vec{\Omega}$) and velocity vector ($\vec{V}$) was less than 40 deg. Above 40 deg, the rotation-balance increments to the aircraft aerodynamic matrix were set equal to zero with an exponential decay function (see Appendix B.3). Under these conditions, the oscillatory rates (p_o, q_o, and r_o) become equal to the total rotational rates (p, q, and r). Likewise, when the total rotational vector ($\vec{\Omega}$) is aligned with the velocity vector ($\vec{V}$), the condition where $\delta = 0$, the aircraft is in a flat spin and the oscillatory rate components are zero.

B.3 ELIMINATION OF DISCONTINUITY EFFECTS WHEN IMPLEMENTING ROTATION-BALANCE DATA

A problem that arises in using the inclination angle criteria is the need to minimize the discontinuity which occurs when the criteria for use of rotary data are satisfied when large rotation rates exist. At such points, significant magnitudes of incremental rotation-balance aerodynamics can be suddenly added into the equation as the rotation vector swings inside of the limiting angle. The addition of this data is instantaneous and is therefore not realistic. To minimize this discontinuity, an exponential decay was used to smoothly bring the incremental rotation-balance data into the equations of motion. By using a small time constant, the exponential function eliminates any pulse effects yet does not reduce the total effect of the rotation-balance data. The technique is outlined below.

$$\Delta C_{m_{rb}} = \Delta C_{m_{rb}} - \Delta C_{m_{smj}} e^{-\Delta t/\tau}$$

where

$$\Delta C_{m_{smj}} = \Delta C_{m_{rbj}} + \Delta C_{m_{smj-1}}$$

$(j$ = time iteration at which enter or exit rotation–balance data $\Delta t = t - t_j)$

$j - 1$ = iteration at previous entry or exit

τ = Washout time constant

$\Delta C_{m_{rb}}$ = (is defined in Appendix B.1)

For other moment coefficients, replace "C_m" with "C_ℓ" or "C_n." The above technique was developed and presented in Ref. 15.

APPENDIX C
DETERMINATION OF AERODYNAMIC MOMENTS FROM FLIGHT TEST

In order to determine angular accelerations produced only by aerodynamics,

$$\dot{p}_{AERO} = \frac{M_X}{I_X}$$

$$\dot{q}_{AERO} = \frac{M_Y}{I_Y}$$

$$\dot{r}_{AERO} = \frac{M_Z}{I_Z}$$

the inertial and engine effects were subtracted from the calculated body axis accelerations (slope of measured body axis angular rates).

$$\dot{p}_{AERO} = \dot{p} - \frac{I_Y - I_Z}{IX} qr - \frac{I_{XZ}}{I_X} (\dot{r} + pq)$$

$$\dot{q}_{AERO} = \dot{q} - \frac{I_Z - I_X}{I_Y} pr - \frac{I_{XZ}}{I_Y} (r^2 - p^2) - \frac{1}{I_Y} \left(M_{Y_T} + M_{Y_G}\right)$$

$$\dot{r}_{AERO} = \dot{r} - \frac{I_X - I_Y}{I_Z} pq - \frac{I_{XZ}}{I_Z} (\dot{p} - qr) - \frac{1}{I_Z} \left(M_{Z_G}\right)$$

The pitch-, roll-, and yawing-moment coefficients attributable to all aerodynamic terms are

$$(C_m)_{AERO} = \frac{\dot{q}_{AERO} I_Y}{\bar{q} SC}$$

$$(C_\ell)_{AERO} = \frac{\dot{p}_{AERO} I_X}{\bar{q} Sb}$$

$$(C_n)_{AERO} = \frac{\dot{r}_{AERO} I_Z}{\bar{q} Sb}$$

NOMENCLATURE

b	Wingspan, ft
C	Wing mean aerodynamic chord, ft
CGNEW	New center-of-gravity location, percent chord
CGREF	Reference center-of-gravity location, percent chord
C_ℓ	Rolling-moment coefficient, rolling moment/$\bar{q}$Sb about airplane cg
C_{ℓ_p}	Derivative of rolling-moment coefficient with respect to roll rate, $\partial C_\ell/\partial(pb/2V)$, per radian
C_{ℓ_q}	Derivative of rolling-moment coefficient with respect to pitch rate, $\partial C_\ell/\partial(qC/2V)$, per radian
C_{ℓ_r}	Derivative of rolling-moment coefficient with respect to yaw rate, $\partial C_\ell/\partial(rb/2V)$, per radian
$C_{\ell_{\dot\beta}}$	Derivative of rolling-moment coefficient with respect to $\dot\beta$, $\partial C_\ell/\partial(\dot\beta b/2V)$, per radian
C_m	Pitching-moment coefficient, pitching moment/$\bar{q}$SC about airplane cg
C_{m_p}	Derivative of pitching-moment coefficient with respect to roll rate, $\partial C_m/\partial(pb/2V)$, per radian
C_{m_q}	Derivative of pitching-moment coefficient with respect to pitch rate, $\partial C_m/\partial(qC/2V)$, per radian
C_{m_r}	Derivative of pitching-moment coefficient with respect to yaw rate, $\partial C_m/\partial(rb/2V)$, per radian
$C_{m_{\dot\alpha}}$	Derivative of pitching-moment coefficient with respect to $\dot\alpha$, $\partial C_m/\partial(\dot\alpha C/2V)$, per radian
C_n	Yawing-moment coefficient, yawing moment/$\bar{q}$Sb about airplane cg
C_{n_p}	Derivative of yawing-moment coefficient with respect to roll rate, $\partial C_n/\partial(pb/2V)$, per radian
C_{n_q}	Derivative of yawing-moment coefficient with respect to pitch rate, $\partial C_n/\partial(qC/2V)$, per radian

C_{n_r} Derivative of yawing-moment coefficient with respect to yaw rate, $\partial C_n/\partial(rb/2V)$, per radian

$C_{n_{\dot{\beta}}}$ Derivative of yawing-moment coefficient with respect to $\dot{\beta}$, $\partial C_n/\partial(\dot{\beta}b/2V)$, per radian

C_x Longitudinal-force coefficient, longitudinal force/$\bar{q}S$

C_{x_q} Derivative of longitudinal-force coefficient with respect to pitch rate, $\partial C_x/\partial(qC/2V)$, per radian

$C_{x_{\dot{\alpha}}}$ Derivative of longitudinal-force coefficient with respect to $\dot{\alpha}$, $\partial C_x/\partial(\dot{\alpha}C/2V)$, per radian

C_y Side-force coefficient, side force/$\bar{q}S$

C_{y_p} Derivative of side-force coefficient with respect to roll rate, $\partial C_Y/\partial(pb/2V)$, per radian

C_{y_r} Derivative of side-force coefficient with respect to yaw rate, $\partial C_Y/\partial(rb/2V)$, per radian

$C_{y_{\dot{\beta}}}$ Derivative of side-force coefficient with respect to $\dot{\beta}$, $\partial C_Y/\partial(\dot{\beta}b/2V)$, per radian

C_z Normal-force coefficient, normal force/$\bar{q}S$

C_{z_q} Derivative of normal-force coefficient with respect to pitch rate, $\partial C_z/\partial(qC/2V)$, per radian

$C_{z_{\dot{\alpha}}}$ Derivative of normal-force coefficient with respect to $\dot{\alpha}$, $\partial C_z/\partial(\dot{\alpha}C/2V)$, per radian

cg Center-of-gravity location, percent chord

d Distance from thrust line to center of gravity

F_X Force acting along X-body axis, lb

F_Y Force acting along Y-body axis, lb

F_Z Force acting along Z-body axis, lb

g Acceleration of gravity, ft/sec^2

h	Altitude, ft
I_X, I_Y, I_Z	Moments of inertia about X-, Y-, and Z-body axes, respectively, slug-ft^2
I_{XZ}	Product of inertia, slug-ft^2
I_{XE}	Moment of inertia about X-body axis due to engine rotation, slug-ft^2
$\vec{i}, \vec{j}, \vec{k}$	Unit vectors along X-, Y-, and Z-body axes, respectively
k	Frequency parameter, $\Omega b/2V$ or $\Omega C/2V$
LPSC	Left pro-spin controls
M_∞	Mach number
M_X	Moment acting about X-body axis, ft-lb
M_Y	Moment acting about Y-body axis, ft-lb
M_{YG}	Moment acting about Y-body axis caused by engine rotation, ft-lb
M_{YT}	Moment acting about Y-body axis caused by engine thrust, ft-lb
M_Z	Moment acting about Z-body axis, ft-lb
M_{ZG}	Moment acting about Z-body axis caused by engine thrust, ft-lb
m	Mass, slugs
p, q, r	Components of $\vec{\Omega}$ about X-, Y-, and Z-body axes, respectively, rad/sec
$\dot{p}_{AERO}$	Aerodynamic contribution to $\dot{p}$, deg/sec^2
$\dot{q}_{AERO}$	Aerodynamic contribution to $\dot{q}$, deg/sec^2
$\dot{r}_{AERO}$	Aerodynamic contribution to $\dot{r}$, deg/sec^2
p_o, q_o, r_o	Components of $\vec{\Omega}$ about X-, Y-, and Z-body axes caused by oscillations superimposed on steady rotation, rad/sec
p_{ss}, q_{ss}, r_{ss}	Components of $\vec{\Omega}_{ss}$ about X-, Y-, and Z-body axes, respectively, rad/sec
$\bar{q}$	Dynamic pressure, $\rho V^2/2$, lb/ft^2

Re_ℓ	Reynolds number based on model length
RDELCG	Moment arm for X axis center-of-gravity transfer, ft
rpm	Revolutions per minute
S	Wing reference area, ft^2
T	Engine thrust, lb
T_X	Component of thrust along X-body axis, lb
T_Y	Component of thrust along Y-body axis, lb
T_Z	Component of thrust along Z-body axis, lb
t	Time, sec
u,v,w	Components of total velocity along X-, Y-, and Z-body axes, respectively, ft/sec
V	Total velocity, ft/sec
X,Y,Z	Body axes
x,y,z	Linear distance along X-, Y-, and Z-body axes, respectively, ft
α	Angle of attack, deg
β	Angle of sideslip, deg
γ	Flight path angle, deg
δ	Angle between rotation vector $\vec{\Omega}$ and the velocity vector, $\vec{V}$, deg
δ_a	Aileron deflection, positive when trailing edge of right aileron is down, deg
δ_H	Elevator deflection, positive when trailing edge is down, deg
δ_r	Rudder deflection, positive when trailing edge is left, deg
ϵ	Angle between thrust line and X-body axis, deg
θ	Angle between X-body axis and horizontal measured in vertical plane, deg

ρ	Air density, slug/ft^3
τ	Time constant
Δt	Incremental time
ϕ	Angle between Y-body axis and horizontal measured in vertical plane, deg
ϕ_E	Engine rotor angular velocity, rad/sec
ψ	Angle between Y-body axis and vertical measured in horizontal plane, deg
$\vec{\Omega}$	Resultant angular vector, rad/sec
$\Omega b/2V$	Nondimensional rotation rate
$\vec{\Omega}_{ss}$	Steady-state angular velocity (component of $\vec{\Omega}$ along velocity vector), rad/sec

SUBSCRIPTS

rb	Indicates rotation-balance data
sp	Short period

SUPERSCRIPT

	Derivative with respect to time